

1 **Role of jellyfish in the plankton ecosystem revealed using a**  
2 **global ocean biogeochemical model**

3 Rebecca M. Wright<sup>1,2</sup>, Corinne Le Quéré<sup>1</sup>, Erik Buitenhuis<sup>1</sup>, Sophie Pitois<sup>2</sup>, Mark Gibbons<sup>3</sup>

4 <sup>1</sup>Tyndall Centre for Climate Change Research, School of Environmental Sciences, University of East Anglia,  
5 Norwich, NR4 7TJ, UK

6 <sup>2</sup>Centre for Environment, Fisheries & Aquaculture Science, Lowestoft, NR33 0HT, UK

7 <sup>3</sup>Department of Biodiversity and Conservation Biology, University of the Western Cape, Cape Town, Bellville  
8 7535, RSA

9

10 *Correspondence to:* Rebecca M. Wright (rebecca.wright@uea.ac.uk)

11

12 **Abstract.** Jellyfish are increasingly recognised as important components of the marine ecosystem, yet their  
13 specific role is poorly defined compared to that of other zooplankton groups. This paper presents the first global  
14 ocean biogeochemical model that includes an explicit representation of jellyfish and uses the model to gain insight  
15 into the influence of jellyfish on the plankton community. The PlankTOM11 model groups organisms into  
16 Plankton Functional Types (PFT). The jellyfish PFT is parameterised here based on our synthesis of observations  
17 on jellyfish growth, grazing, respiration and mortality rates as functions of temperature and on jellyfish biomass.  
18 The distribution of jellyfish is unique compared to that of other PFTs in the model. The jellyfish global biomass  
19 of 0.13 PgC is within the observational range, and comparable to the biomass of other zooplankton and  
20 phytoplankton PFTs. The introduction of jellyfish in the model has a large direct influence on the crustacean  
21 macrozooplankton PFT and influences indirectly the rest of the plankton ecosystem through trophic cascades. The  
22 zooplankton community in PlankTOM11 is highly sensitive to the jellyfish mortality rate, with jellyfish  
23 increasingly dominating the zooplankton community as its mortality diminishes. Overall, the results suggest that  
24 jellyfish play an important role in regulating global marine plankton ecosystems, [across plankton community](#)  
25 [structure, spatiotemporal dynamics, and biomass, a role](#) which has been generally neglected so far.

Deleted: ,

26

## 28 1 INTRODUCTION

29

30 Gelatinous zooplankton are increasingly recognised as influential organisms in the marine environment, not just  
31 for the disruptions they can cause to coastal economies (fisheries, aquaculture, beach closures and power plants  
32 etc.; Purcell et al., 2007), but also as important consumers of plankton (Lucas and Dawson, 2014), a food source  
33 for many marine species (Lamb et al., 2017) and as key components in marine biogeochemical cycles (Crum et  
34 al., 2014; Lebrato et al., 2012). The term gelatinous zooplankton can encompass a wide range of organisms across  
35 three phyla: Tunicata (salps), Ctenophora (comb-jellies), and Cnidaria (true jellyfish). This study focuses on  
36 Cnidaria (including Hydrozoa, Cubozoa and Scyphozoa), which contribute 92% of the total global biomass of  
37 gelatinous zooplankton (Lucas et al., 2014). The other gelatinous zooplankton groups, Tunicata and Ctenophora,  
38 are excluded from this study because there ~~is~~ <sup>is</sup> far ~~less~~ <sup>less</sup> data available on their biomass and vital rates than for  
39 Cnidaria, and they only contribute a combined global biomass of 8% of total gelatinous zooplankton (Lucas et al.,  
40 2014). Cnidaria are both independent enough from other gelatinous zooplankton, and cohesive enough to be  
41 represented as a single Plankton Functional Type (PFT) for global modelling (Le Quéré et al., 2005). For the rest  
42 of this paper pelagic Cnidaria are referred to as jellyfish.

43 Jellyfish exhibit a radially symmetrical body plan and are characterised by a bell-shaped body (medusae).  
44 Swimming is achieved by muscular, “pulsing” contractions and animals have one opening for both feeding and  
45 excretion. Most scyphozoans and cubozoans, and many hydrozoans, follow a meroplanktonic life cycle. A sessile  
46 (generally) benthic polyp buds off planktonic ephyrae asexually. These, in turn, grow into medusae that reproduce  
47 sexually to generate planula larvae, which then settle and transform into polyps. Within this general life cycle,  
48 there is large reproductive and life cycle variety, including some holoplanktonic species that skip the benthic  
49 polyp stage as well as holobenthic species that skip the pelagic phase, and much plasticity (Boero et al., 2008;  
50 Lucas and Dawson, 2014).

51 Jellyfish are significant consumers of plankton, feeding mostly on zooplankton using tentacles and/or oral arms  
52 containing stinging cells called nematocysts (Lucas and Dawson, 2014). The large body size to carbon content  
53 ratio of jellyfish creates a low maintenance, large feeding structure, which, because they do not use sight to capture  
54 prey, allow them to efficiently clear plankton throughout 24 hours (Acuña et al., 2011; Lucas and Dawson, 2014).  
55 Jellyfish are connected to lower trophic levels, with the ability to influence the plankton ecosystem structure and  
56 thus the larger marine ecosystem through trophic cascades (Pitt et al., 2007, 2009; West et al., 2009). Jellyfish  
57 have the ability to rapidly form large high-density aggregations known as blooms that can temporarily dominate  
58 local ecosystems (Graham et al., 2001; Hamner and Dawson, 2009). Jellyfish contribute to the biogeochemical  
59 cycle through two main routes; from life through feeding processes, including the excretion of faecal pellets,  
60 mucus and messy-eating, and from death, through the sinking of carcasses (Chelsky et al., 2015; Lebrato et al.,  
61 2012, 2013a; Pitt et al., 2009). The high biomass achieved during jellyfish blooms, and the rapid sinking of  
62 excretions from feeding and carcasses from such blooms, make them a potentially significant vector for carbon  
63 export (Lebrato et al., 2013a, 2013b; Luo et al., 2020).

64 Anthropogenic impacts from climate change, such as increasing temperature and acidity (Rhein et al., 2013), and  
65 fishing, through the removal of predators and competitors (Doney et al., 2012), impact the plankton including

Deleted: are

Deleted: fewer

68 jellyfish (Boero et al., 2016; but see Richardson and Gibbons, 2008). Multiple co-occurring impacts make it  
69 difficult to understand the role of jellyfish in the marine ecosystem, and how the role may be changed by the co-  
70 occurring impacts. The paucity of historical jellyfish biomass data, especially outside of coastal regions and the  
71 Northern Hemisphere, has made it difficult to establish jellyfish global spatial distribution, biomass and trends  
72 from observations (Brotz et al., 2012; Condon et al., 2012; Gibbons and Richardson, 2013; Lucas et al., 2014; Pitt  
73 et al., 2018).

74 Models are useful tools to help understand the interactions of multiple complex drivers in the environment. This  
75 paper describes the addition of jellyfish to the PlankTOM10 global ocean biogeochemical model, which we call  
76 PlankTOM11. PlankTOM10 represents explicitly 10 PFTs; six phytoplankton, one bacteria and three zooplankton  
77 (Le Quéré et al., 2016). The three zooplankton groups are protozooplankton (mainly heterotrophic flagellates and  
78 ciliates), mesozooplankton (mainly copepods) and macrozooplankton (as crustaceans, mainly euphausiids; see  
79 Table 1 for definitions). Jellyfish is therefore the fourth zooplankton group and 11<sup>th</sup> PFT in the PlankTOM model  
80 series. It introduces an additional trophic level to the ecosystem. To our knowledge, this is the first and only  
81 representation of jellyfish in a global ocean biogeochemical model at the time of writing. PlankTOM11 is used to  
82 help quantify global jellyfish biomass and the role of jellyfish for the global plankton ecosystem.

## 83 2 METHODS

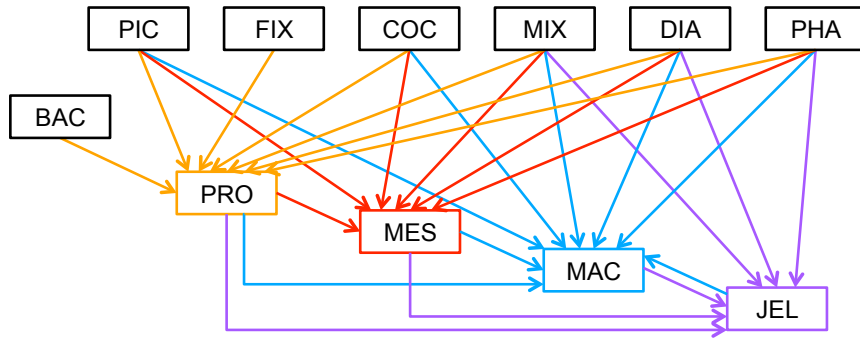
### 84 2.1 PLANKTOM11 MODEL DESCRIPTION

85

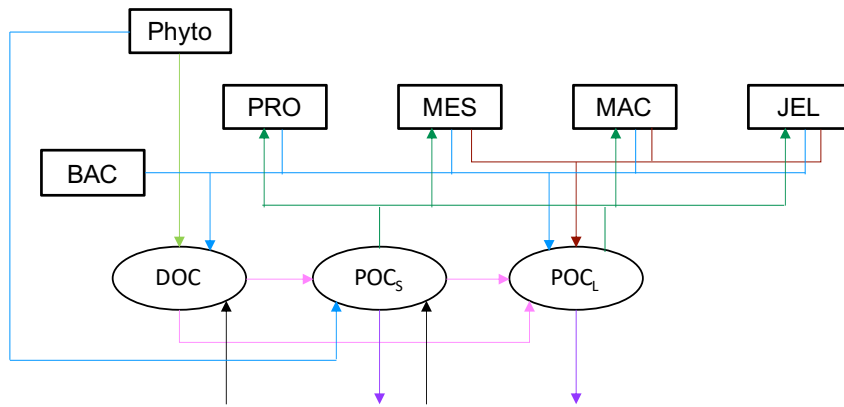
86 PlankTOM11 was developed starting from the 10 PFT version of the PlankTOM model series (Le Quéré et al.,  
87 2016), by introducing jellyfish as an additional trophic level at the top of the plankton food web (Fig. 1a). A full  
88 description of PlankTOM10 is published in Le Quéré et al. (2016), including all equations and parameters. Here  
89 we provide an overview of the model development, focussing on the parameterisation of the growth and loss rates  
90 of jellyfish and how these compare to the other macrozooplankton group. We also describe the update of the  
91 relationship used to describe the growth rate as a function of temperature and subsequent tuning. The formulation  
92 of the growth rate is the only equation that has changed since the previous version of the model (Le Quéré et al.,  
93 2016), although many parameters have been modified (Sect. 2.1.6).

94 PlankTOM11 is a global ocean biogeochemistry model that simulates plankton ecosystem processes and their  
95 interactions with the environment through the representation of 11 PFTs (Fig. 1). The 11 PFTs consist of six  
96 phytoplankton (picophytoplankton, nitrogen-fixing cyanobacteria, coccolithophores, mixed phytoplankton,  
97 diatoms and *Phaeocystis*), bacteria, and four zooplankton (Table 1). Physiological parameters are fixed within  
98 each PFT, and therefore, within-PFT diversity is not included. Spatial variability within PFTs is represented  
99 through parameter-dependence on environmental conditions including temperature, nutrients, light and food  
100 availability.

(a) Plankton food web



(b) Sources and sinks for organic carbon



- > mortality
- > primary production
- > egestion & excretion
- > deposition (river, dust & air)
- > aggregation
- > grazing
- > sinking

101

102 Figure 1. Schematic representation of the PlankTOM11 marine ecosystem model (see Table 1 for PFT definitions). (a) The  
 103 plankton food web, arrows represent the grazing fluxes by protozooplankton (orange), mesozooplankton (red),  
 104 macrozooplankton (blue) and jellyfish zooplankton (purple). Only fluxes with relative preferences above 0.1 are shown (see  
 105 Table 3). (b) Source and sinks for dissolved organic carbon (DOC) and small (POC<sub>s</sub>) and large (POC<sub>L</sub>) particulate organic carbon.

106

107 The model contains 39 biogeochemical tracers, with full marine cycles of key elements carbon, oxygen,  
 108 phosphorus and silicon, and simplified cycles of nitrogen and iron. There are three detrital pools: dissolved organic

109 carbon (DOC), small particulate organic carbon (POCs) and large particulate organic carbon (POC<sub>L</sub>). The  
 110 elements enter through riverine fluxes and are cycled and generated through the PFTs via feeding, faecal matter,  
 111 messy-eating and carcasses (Fig. 1b; see Sect. 2.1.5. for detail; Buitenhuis et al., 2006, 2010, 2013a; Le Quéré et  
 112 al., 2016). Model parameters are based on observations where available. A global database of PFT carbon biomass  
 113 that was designed for model studies (Buitenhuis et al., 2013b) and global surface chlorophyll from satellite  
 114 observations (SeaWiFS) are used to guide the model developments.

**Table 1.** Size range and descriptions of PFT groups used in PlankTOM11. Adapted from Le Quéré et al. (2016).

Name	Abbreviation	Size Range $\mu\text{m}$	Description/Includes
<b>Autotrophs</b>			
Pico-phytoplankton	PIC	0.5 – 2	Pico-eukaryotes and non N <sub>2</sub> -fixing cyanobacteria such as <i>Synechococcus</i> and <i>Prochlorococcus</i>
N <sub>2</sub> -fixers	FIX	0.7 – 2	<i>Trichodesmium</i> and N <sub>2</sub> -fixing unicellular cyanobacteria
Coccolithophores	COC	5 – 10	
Mixed-phytoplankton	MIX	2 – 200	e.g. autotrophic dinoflagellates and chrysophytes
Diatoms	DIA	20 – 200	
<i>Phaeocystis</i>	PHA	120 – 360	Colonial <i>Phaeocystis</i>
<b>Heterotrophs</b>			
Bacteria	BAC	0.3 – 1	Here used to subsume both heterotrophic <i>Bacteria</i> and <i>Archaea</i>
Protozooplankton	PRO	5 – 200	e.g. heterotrophic flagellates and ciliates
Mesozooplankton	MES	200 – 2000	Predominantly copepods
Macrozooplankton	MAC	>2000	Euphausiids, amphipods, and others, known as crustacean macrozooplankton
Jellyfish zooplankton	JEL	200 – >20,000	Cnidaria medusae, ‘true jellyfish’

115

116 The PlankTOM11 marine biogeochemistry component is coupled online to the global ocean general circulation  
 117 model Nucleus for European Modeling of the Ocean version 3.5 (NEMO v3.5). We used the global configuration  
 118 with a horizontal resolution of 2° longitude by a mean resolution of 1.1° latitude using a tripolar orthogonal grid.  
 119 The vertical resolution is 10m for the top 100m, decreasing to a resolution of 500m at 5km depth, and a total of

120 30 vertical z-levels (Madec, 2013). The ocean is described as a fluid using the Navier-Stokes equations and a  
 121 nonlinear equation of state (Madec, 2013). NEMO v3.5 explicitly calculates vertical mixing at all depths using a  
 122 turbulent kinetic energy model and sub-grid eddy induced mixing. The model is interactively coupled to a  
 123 thermodynamic sea-ice model (LIM version 2; Timmermann et al., 2005).

124 The temporal ( $t$ ) evolution of zooplankton concentration ( $Z_j$ ), including the jellyfish PFT, is described through  
 125 the formulation of growth and loss rates as follows:

$$126 \frac{\partial Z_j}{\partial t} = \sum_k g_{F_k}^{Z_j} \times F_k \times MGE \times Z_j - \sum_{k=1}^4 g_{Z_j}^{Z_k} \times Z_k \times Z_j - R_{0^\circ}^{Z_j} \times d_{Z_j}^T \times Z_j \quad (1)$$

127 *growth through grazing – loss through grazing – basal respiration*

$$128 - m_{0^\circ}^{Z_j} \times c_{Z_j}^T \times \frac{Z_j}{K_{1/2}^{Z_j} + Z_j} \times \sum_i P_i$$

129 *– mortality*

130 For growth through grazing,  $g_{F_k}^{Z_j}$  is the grazing rate by zooplankton  $Z_j$  on food source  $F_k$ . This is a temperature-  
 131 dependent Michaelis-Menten term that includes grazing preference (see Sect. 2.1.2.).  $MGE$  is the modelled growth  
 132 efficiency (Buitenhuis et al., 2010). For loss through grazing,  $g_{Z_j}^{Z_k}$  is the grazing of other zooplankton on  $Z_j$ . For  
 133 basal respiration,  $R_{0^\circ}^{Z_j}$  is the respiration rate at  $0^\circ\text{C}$ ,  $T$  is temperature,  $d_{Z_j}$  is the temperature dependence of  
 134 respiration ( $d^{10} = Q_{10}$ ). Mortality is the closure term of the model and is mostly due to predation by higher trophic  
 135 levels than are represented by the model.  $m_{0^\circ}^{Z_j}$  is the mortality rate at  $0^\circ\text{C}$ ,  $c_{Z_j}$  is the temperature dependence of  
 136 the mortality ( $c^{10} = Q_{10}$ ) and  $K_{1/2}^{Z_j}$  is the half saturation constant for mortality.  $\sum_i P_i$  is the sum of all PFTs,  
 137 excluding bacteria, and is used as a proxy for the biomass of predators not explicitly included in the model. More  
 138 details on each term are provided below and parameter values are given in Tables 2 through 5.

139

### 140 2.1.1 PFT Growth

141

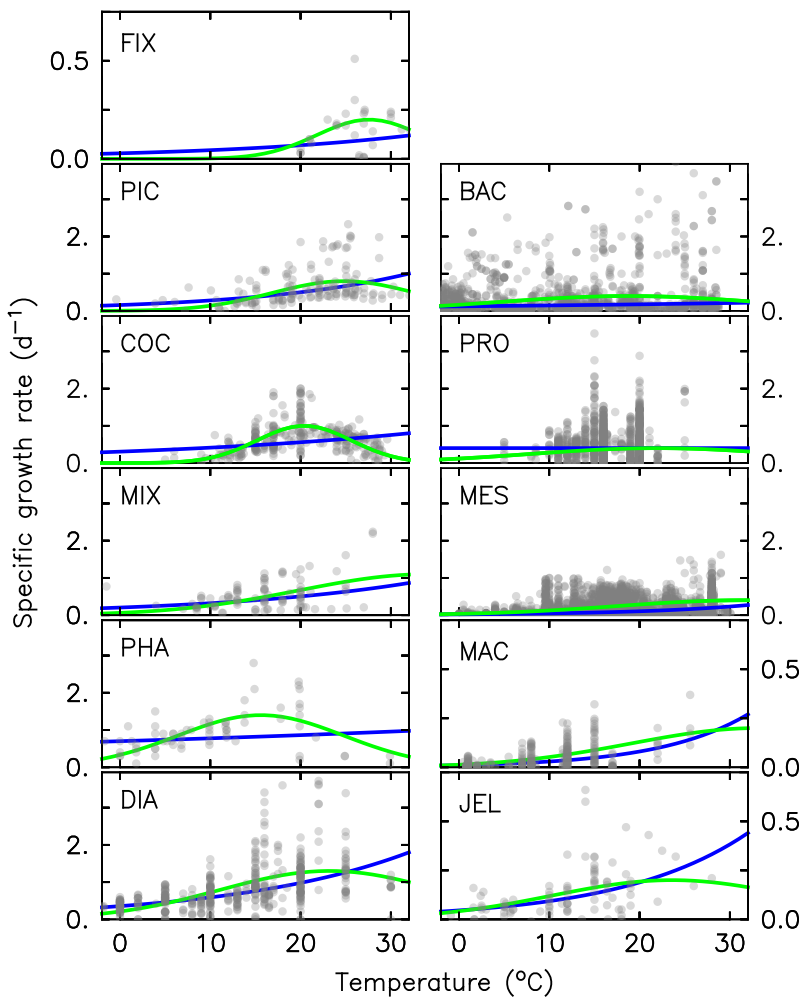
142 Growth rate is the trait that most distinguishes PFTs in models (Buitenhuis et al., 2006, 2013a). Jellyfish growth  
 143 rates were compiled as a function of temperature from the literature (see Appendix Table A1). In previous  
 144 published versions of the PlankTOM model, growth as a function of temperature ( $\mu^T$ ) was fitted with two  
 145 parameters:

$$146 \mu^T = \mu_0 \times Q_{10}^{\frac{T}{10}} \quad (2)$$

147 where  $\mu_0$  is the growth at  $0^\circ\text{C}$ ,  $Q_{10}$  is the temperature dependence of growth derived from observations, and  $T$  is  
 148 the temperature (Le Quéré et al., 2016). Jellyfish growth rate is poorly captured by an exponential fit to  
 149 temperature. To better capture the observations, the growth calculation has now been updated with a three-  
 150 parameter growth rate, which produces a bell-shaped curve centred around an optimal growth rate at a given  
 151 temperature (Fig. 2 and Table 2). The three-parameter fit is suitable for the global modelling of plankton because

152 it can represent an exponential increase if the data support this (Schoemann et al., 2005). The growth rate as a  
 153 function of temperature ( $\mu^T$ ) is now defined by; the optimal temperature ( $T_{opt}$ ), maximum growth rate ( $\mu_{max}$ ) at  
 154  $T_{opt}$ , and the temperature interval ( $dT$ ):

155 
$$\mu^T = \mu_{max} \times \exp\left[\frac{-(T - T_{opt})^2}{dT^2}\right] \quad (3)$$



156

157 *Figure 2. Maximum growth rates for the 11 PFTs as a function of temperature from observations (grey circles). The three-*  
 158 *parameter fit to data is shown in green and the two-parameter fit is shown in blue, using the parameter values from Table 2.*  
 159 *For full PFT names see Table 1. The R<sup>2</sup> for both fits to data are given in Appendix Table A2.*

Deleted: the

Deleted: the



**Table 2.** Parameters used to calculate PFT specific growth rate with three-parameter fit (Eq. 3) in PlankTOM11.

PFT	$\mu_{\max}$ (d <sup>-1</sup> )	T <sub>opt</sub> (°C)	dT (°C)
FIX	0.2	27.6	8.2
PIC	0.8	24.8	11.2
COC	1.0	20.4	7.4
MIX	1.1	34.0	20.0
PHA	1.4	15.6	13.0
DIA	1.3	23.2	17.2
BAC	0.4	18.8	20.0
PRO	0.4	22.0	20.0
MES	0.4	31.6	20.0
MAC	0.2	33.2	20.0
JEL	0.2	23.6	18.8

162

163 The available observations measure growth rate, but the model requires specification of the grazing rate (Eq. 1).

164 Growth of zooplankton and grazing ( $g^T$ ) are related through the gross growth efficiency (GGE):

165 
$$g^T = \frac{u^T}{GGE} \quad (4)$$

166 GGE is the portion of grazing that is converted to biomass. This was previously collated by Moriarty (2009) from

167 the literature for crustacean and gelatinous macrozooplankton for the development of PlankTOM10. We extracted

168 data for jellyfish from this collation (all scyphomedusae) which gave an average GGE of  $0.29 \pm 0.27$ , n=126

169 (Moriarty, 2009).

170

### 171 2.1.2 Jellyfish PFT Grazing

172

173 The food web, and thus the trophic level of PFTs is determined through grazing preferences. The relative

174 preference of jellyfish zooplankton for the other PFTs was determined through a literature search (Colin et al.,

175 2005; Costello and Colin, 2002; Flynn and Gibbons, 2007; Malej et al., 2007; Purcell, 1992, 1997, 2003; Stoecker

Deleted: the

177 et al., 1987; Uye and Shimauchi, 2005a; see Appendix Table A3 for further detail). The dominant food source  
 178 was mesozooplankton (specifically copepods), followed by proto-zooplankton (most often ciliates) and then  
 179 macrozooplankton (Table 3). There is little evidence in the literature for jellyfish actively consuming autotrophs.  
 180 One of the few pieces of evidence is a gut content analysis where ‘unidentified protists... some chlorophyll  
 181 bearing’ were found in a small medusa species (Colin et al., 2005). Another is a study by Boero et al. (2007)  
 182 which showed that very small medusae such as *Obelia* will consume bacteria and may consume phytoplankton.  
 183 Studies on the diet of the ephyrae life cycle stage are limited in comparison to those on medusa, but the literature  
 184 does show evidence for ephyrae consuming protists and phytoplankton (Båmstedt et al., 2001; Morais et al., 2015).  
 185 We assume that ephyrae are likely to have a higher preference for autotrophs, due to their smaller size as with the  
 186 small medusa, but that this will have a minimal effect on the overall preferences and the biomass consumed, so  
 187 preferences for autotrophs are kept low. Once the relative preference is established, the absolute value of the  
 188 preference is tuned to improve the biomass of the different PFTs, as in Le Quéré et al. (2016). Table 3 shows the  
 189 relative preference of jellyfish for its prey assigned in the model, along with the preferences of the other  
 190 zooplankton PFTs. The zooplankton relative preferences are based around a predator-prey size ratio, which by  
 191 design is set to 1 for zooplankton-diatom. Preferences to other PFTs and to particulate carbon are then set relative  
 192 to the preference for diatoms. The preference ratios are weighted using the global carbon biomass for each type  
 193 against a total food biomass weighted mean (sum of all the PFTs), calculated from the MAREDAT database,  
 194 following the methodology used for the other PFTs (Buitenhuis et al., 2013a; Le Quéré et al., 2016). Zooplankton  
 195 grazing is calculated using:

$$196 \quad g_{F_k}^{Z_j} = \mu^T \frac{p_{F_k}^{Z_j}}{K_{1/2}^{Z_j} + \sum p_{F_k}^{Z_j} F_k} \quad (5)$$

197 where  $g_{F_k}^{Z_j}$  is the grazing rate by zooplankton  $Z_j$  on food source  $F_k$  as shown in Eq. 1, where  $\mu^T$  is the growth rate  
 198 of zooplankton (Eq. 3),  $p_{F_k}^{Z_j}$  is the preference of the zooplankton for the food source (prey) and  $K_{1/2}^{Z_j}$  is the half  
 199 saturation constant of zooplankton grazing. The parameter values for grazing used in the model are given in Table  
 200 4.

201

### 202 2.1.3 Jellyfish PFT Respiration

203

204 Previous analysis of respiration rates of jellyfish found that temperature manipulation experiments with  $Q_{10}$  values  
 205 of  $>3$  were flawed because the temperature was changed too rapidly (Purcell, 2009; Purcell et al., 2010). In a  
 206 natural environment, jellyfish gradually acclimate to temperature changes which has a smaller effect on their  
 207 respiration rates. Purcell et al. (2010) instead collated values from experiments that measured respiration at  
 208 ambient temperatures, providing a range of temperature data across different studies. They found that  $Q_{10}$  for  
 209 respiration was 1.67 for *Aurelia* species (Purcell, 2009; Purcell et al., 2010). Moriarty (2009) collated a respiration  
 210 dataset for zooplankton, including gelatinous zooplankton, using a similar selectivity as Purcell et al. (2010) for  
 211 experimental temperature, feeding, time in captivity and activity levels. Jellyfish were extracted from the Moriarty

**Table 3.** Relative preference, expressed as a ratio, of zooplankton for food (grazing) used in PlankTOM11. For each zooplankton the preference ratio for diatoms is set to 1.

PFT	PRO	MES	MAC	JEL
<b>Autotrophs</b>				
FIX	2	0.1	0.1	0.1
PIC	3	0.75	0.5	0.1
COC	2	0.75	1	0.1
MIX	2	0.75	1	1
DIA	1	1	1	1
PHA	2	1	1	1
<b>Heterotrophs</b>				
BAC	4	0.1	0.1	0.1
PRO	0	2	1	7.5
MES	0	0	2	10
MAC	0	0	0	5
JEL	0	0	0.5	0
<b>Particulate matter</b>				
Small organic particles	0.1	0.1	0.1	0.1
Large organic particles	0.1	0.1	0.1	0.1

212

213 (2009) dataset, which also included experiments on non-adult and non-*Aurelia* species medusae, unlike the Purcell  
 214 et al. (2010) dataset. The relationship between temperature and respiration is heavily skewed by body mass  
 215 (Purcell et al., 2010). The data were thus normalised by fitting to a general linear model (GLM) using a least  
 216 squares cost function, to reduce the effect of body mass on respiration rates (Ikeda, 1985; Le Quéré et al., 2016).

217  $GLM = \log_{10}RR = a + b \log_{10}BM + c T$  (6)

218

219 
$$cost\ function = \sum \left( \frac{R_{GLM}^T - R_{Obs}^T}{R_{Obs}^T} \right)^2 \quad (7)$$

220 Where  $RR$  is the respiration rate,  $BM$  is the body mass, and  $T$  and  $R^T$  are the observed temperature and associated  
 221 respiration rate. The parameters values were then calculated using  $R_0 = e^a$ , and  $Q_{10} = (e^c)^{10}$ , where  $e$  is the  
 222 exponential function. The resulting fit to data is shown in Fig. 3. The parameter values for respiration used in the  
 223 model are given in Table 4. Macrozooplankton respiration values are also given in Fig. 3 and Table 4, to provide  
 224 a comparison to another zooplankton PFT of the most similar size available.

**Table 4.** PlankTOM11 parameter values for macrozooplankton and jellyfish, with the associated equation.

Parameters	JEL	MAC	Equation
Respiration			
$R_0^{Z_j}$ (d <sup>-1</sup> )	0.03	0.01	Eq. 1
$d_{Z_j}$	1.88	2.46	Eq. 1
Mortality			
$m_0^{Z_j}$ (d <sup>-1</sup> )	0.12	0.02	Eq. 1
$c_{Z_j}$	1.20	3.00	Eq. 1
$K^{Z_j}$ (μmol C L <sup>-1</sup> )	20.0e-6	20.0e-6	Eq. 1
GGE	0.29	0.30	Eq. 4
Grazing half saturation constant $K_{1/2}^{Z_j}$ (μmol C L <sup>-1</sup> )	10.0e-6	9.0e-6	Eq. 5

225

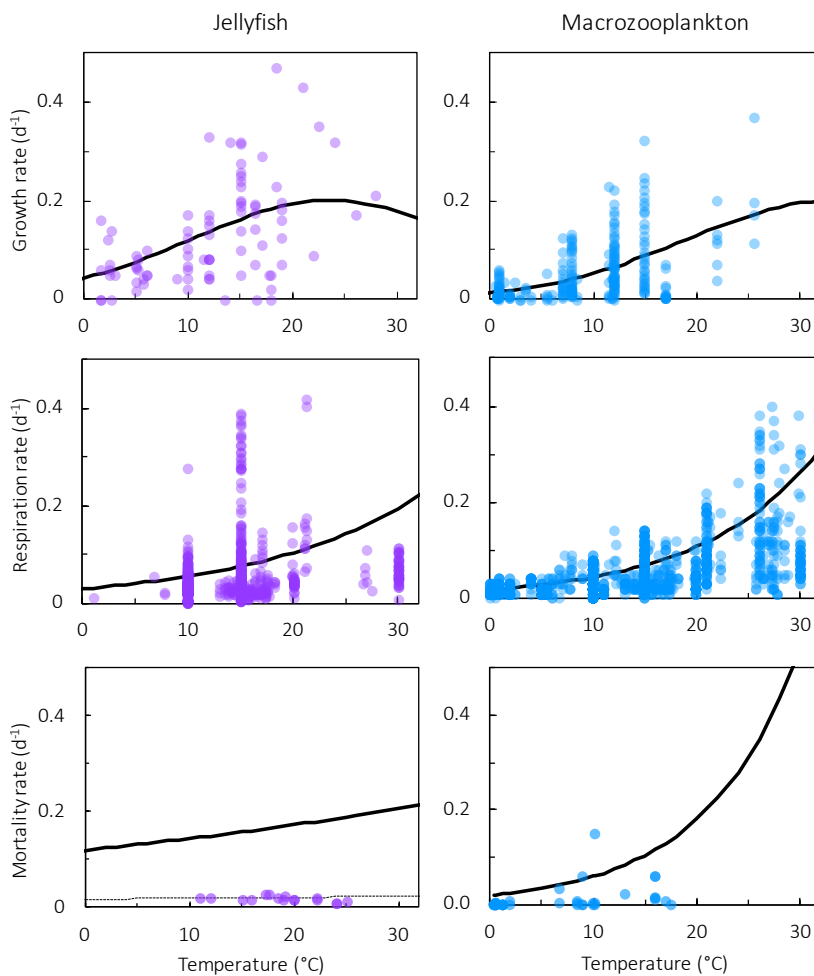
#### 226 2.1.4 Jellyfish PFT Mortality

227

228 There is limited data on mortality rates for jellyfish and to use mortality data from the literature on any  
 229 zooplankton group some assumptions must be made (Acevedo et al., 2013; Almeda et al., 2013; Malej and Malej,  
 230 1992; Moriarty, 2009; Rosa et al., 2013). These assumptions are: that the population is in a steady state where  
 231 mortality equals recruitment, reproduction is constant and that mortality is independent of age (Moriarty, 2009).  
 232 All models with zooplankton mortality rates follow these assumptions. In reality the mortality of a zooplankton  
 233 population is highly variable. Steady states are balanced over a long period (if a population remains viable),  
 234 reproduction is restricted to certain times of year and the early stages of life cycles are many times more vulnerable

235 to mortality. Despite these assumptions, with the limited data on mortality rates, the larger uncertainty lies with  
 236 the data rather than the assumptions (Moriarty, 2009). The half saturation constant for mortality ( $K_{1/2}^{Zj}$  in Eq. 1) is  
 237 set to  $20 \mu\text{mol C L}^{-1}$  the same as other zooplankton types, due to the lack of PFT specific data. In the small amount  
 238 of data available and suitable for use in the model (16 data points from two studies) mortality ranged from 0.006  
 239 – 0.026 per day (Acevedo et al., 2013; Malej and Malej, 1992). Applying the exponential fit to these data gave a  
 240 mortality rate at  $0^\circ\text{C}$  ( $m_0^{Zj}$  in Eq. 1) of 0.018 per day. Sensitivity tests were carried out from this mortality rate  
 241 due to low confidence in the value.

Deleted: i

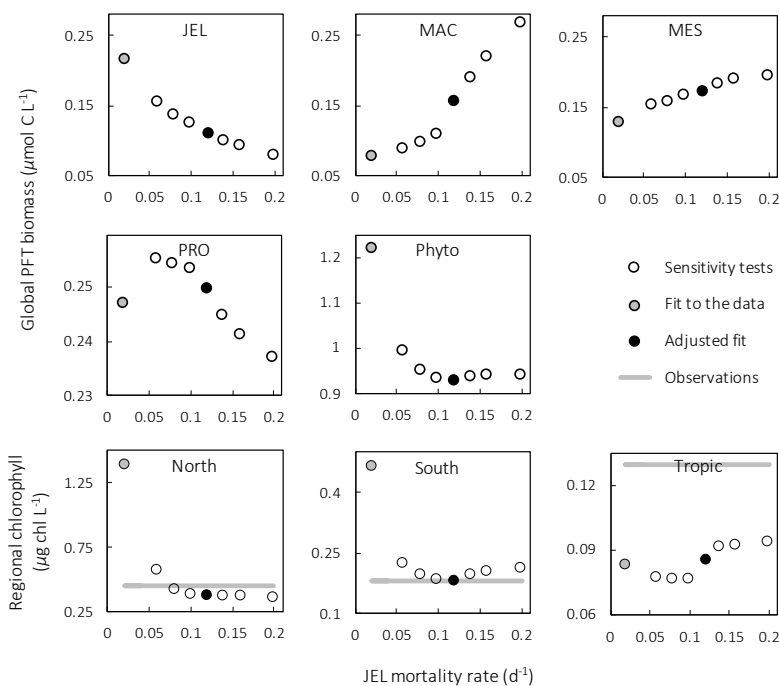


242  
 243 Figure 3. Maximum growth rates (top), respiration rates (middle) and mortality rates (bottom) for jellyfish (left; purple) and  
 244 macrozooplankton (right; blue) PFTs as a function of temperature. The fit to data is shown in black, using the parameter  
 245 values from Table 2 and Table 4. Growth rates are the same as shown in Fig. 2, on a different scale. For jellyfish mortality the  
 246 thin dashed line is the fit to data and the solid line is the adjusted fit (Table 4).

Deleted: the

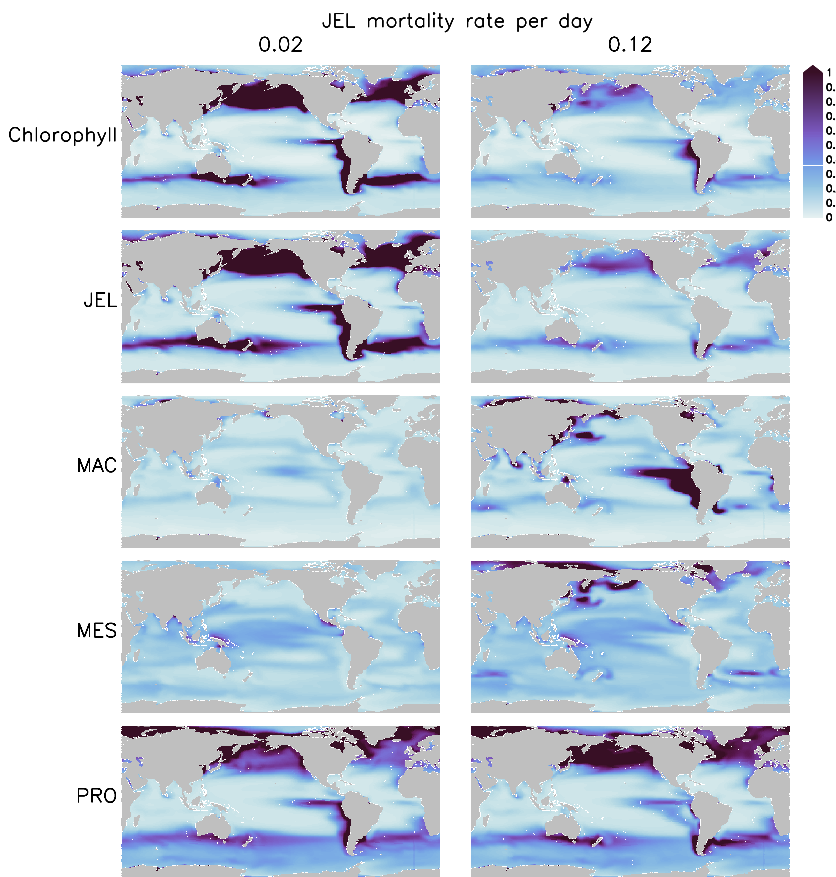
249 Results from a subset of the sensitivity tests are shown in Fig. 4. The model was found to best represent a range  
 250 of observations when jellyfish mortality was increased to 0.12 per day. The fit to [data for mortality](#) ( $\mu_0 = 0.018$ )  
 251 and the adjusted mortality ( $\mu_0 = 0.12$ ) is shown in Fig. 3. This value was chosen based on expert judgement of the  
 252 overall fit across multiple data streams. Whereas it was informed by the quantitative values in Table 6, the final  
 253 choice required the balance of positive and negative performance that required expert judgement rather than a  
 254 statistical number. Mortality rate values closer to 0.018 per day allowed jellyfish to dominate macro- and  
 255 mesozooplankton, greatly reducing their biomass (Fig. 4 and Fig. 5). Low jellyfish mortality also resulted in  
 256 higher chlorophyll concentrations than observed, especially in the high latitudes (Fig. 4 and Fig. 5; Bar-On et al.,  
 257 2018; Buitenhuis et al., 2013b). The adjusted mortality rate used for PlankTOM11 may be accounting for several  
 258 components missing from experimental data including the impact of higher trophic level grazing in the Avecedo  
 259 et al. (2013) study, which in copepods is 3-4 times higher than other sources of mortality (Hirst and Kjørboe,  
 260 2002), the greater vulnerability to mortality experienced during the early stages of the life cycle and mortality due  
 261 to parasites and viruses, especially during blooms (Pitt et al., 2014).

Deleted: for the data



262

263 *Figure 4. Results from sensitivity tests on jellyfish mortality rates. The adjusted fit simulation used for PlankTOM11 is shown*  
 264 *by the black filled circle and the fit to the data simulation is shown by the grey filled circle; global mean PFT biomass ( $\mu\text{mol}$*   
 265  *$\text{C L}^{-1}$ ) for 0-200m depth (top - middle), regional mean surface chlorophyll concentration ( $\mu\text{g chl L}^{-1}$ ; bottom). For the regional*  
 266 *mean chlorophyll the observations are calculated from SeaWiFS. All data are averaged for 1985-2015, and between  $30^{\circ}$*   
 267 *and  $55^{\circ}$  latitude in both hemispheres:  $140\text{-}240^{\circ}\text{E}$  in the north and  $140\text{-}290^{\circ}\text{E}$  in the south (see Fig. 8). Phyto is the sum of all*  
 268 *the phytoplankton PFTs.*



270

271 **Figure 5.** Annual mean surface chlorophyll ( $\mu\text{g chl L}^{-1}$ ) and zooplankton carbon biomasses ( $\mu\text{mol C L}^{-1}$ ) of JEL, MAC, MES and  
 272 PRO for adjustment of JEL mortality for the simulation with  $0.02 \text{ mortality/day}^{-1}$  (left) and the adjusted fit simulation with  
 273  $0.12 \text{ mortality/day}^{-1}$  (right) used in PlankTOM11. Results are shown for the surface box (0-10 meters) and averaged for  
 274 1985-2015.

275 PlankTOM11 uses a mortality rate for jellyfish that is much higher than the limited observations (Fig. 4 and Fig.  
 276 5). Lower jellyfish mortality is likely to be more representative of adult life stages, as jellyfish experience high  
 277 mortality during juvenile life stages, especially as planula larvae and during settling (Lucas et al., 2012). The  
 278 limited observations of jellyfish mortality are from mostly adult organisms, which may explain the dominance of  
 279 jellyfish in the model when parameterised with the observed mortality fit. The higher mortality used for this study  
 280 may be more representative of an average across all life stages. Experimental jellyfish mortality is also likely to  
 281 be lower than *in situ* mortality due to factors such as senescence post-spawning and bloom conditions increasing  
 282 the prevalence of disease and parasites and thus increasing mortality (Mills, 1993; Pitt et al., 2014). Using a higher  
 283 mortality for this study is therefore deemed reasonable.

284

#### 285 2.1.5 Organic Carbon Cycling Through the Plankton Ecosystem

286

287 In PlankTOM11, the growth of phytoplankton modifies dissolved inorganic carbon into DOC, which then  
288 aggregates into POC<sub>s</sub> and POC<sub>L</sub> (Fig. 1b). POC<sub>s</sub> is also generated from protozooplankton egestion and excretion  
289 and is consumed through grazing by all zooplankton. POC<sub>L</sub> is also generated by aggregation from POC<sub>s</sub>, egestion  
290 and excretion by all zooplankton, and from the mortality of mesozooplankton, macrozooplankton and jellyfish,  
291 and is consumed through grazing by all zooplankton. The portion of POC<sub>s</sub> and POC<sub>L</sub> which is not grazed, sinks  
292 through the water column and is counted as export production at 100m (Fig. 1b). The sinking speed of POC<sub>s</sub> is 3  
293 m/d<sup>-1</sup> and the sinking speed of POC<sub>L</sub> varies, depending on the concentration of ballast and the resulting particle  
294 density. Proto-, meso- and macrozooplankton excretion is largely in the form of particulate and solid faecal pellets,  
295 while this makes up very little of jellyfish excretion. Jellyfish instead produce and slough off mucus as part of  
296 their feeding mechanism (Pitt et al., 2009), which is represented in the model in the same way as the faecal pellet  
297 excretion, as a fraction of unassimilated grazing contributing to POC<sub>L</sub>.

298

#### 299 2.1.6 Additional Tuning

300

301 Following the change to the growth rate formulation (from Eq. 2 to Eq. 3), all PFT growth rates are lower  
302 compared to the published version of PlankTOM10 (Le Quéré et al., 2016), but the change is largest for  
303 *Phaeocystis*, diatoms, bacteria and protozooplankton (Fig. 2). Further tuning is carried out to rebalance the total  
304 biomass among phytoplankton PFTs following the change in formulation. The tuning included increasing the  
305 grazing ratio preference of mesozooplankton for *Phaeocystis* and the grazing ratio preference of protozooplankton  
306 for picophytoplankton within the limits of observations. Tuning also included increasing the half saturation  
307 constant of the phytoplankton *Phaeocystis*, picophytoplankton and diatoms for iron. The tuning resulted in a  
308 reduction of *Phaeocystis* biomass and an increase in diatom biomass, without disrupting the rest of the ecosystem.  
309 Diatom respiration was also increased to reduce their biomass towards observations. Finally, bacterial biomass  
310 was increased closer to observations by reducing the half saturation constant of bacteria for dissolved organic  
311 carbon and reducing the maximum bacteria uptake rate. See Appendix Table A4 for the parameter values before  
312 and after tuning.

313 As shown in Eq. 1, there is a component in the mortality of zooplankton to represent predation by organisms not  
314 included in the model. The jellyfish PFT is a significant grazer of macrozooplankton and mesozooplankton (Table  
315 3), to account for this additional grazing the mortality term for macrozooplankton and the respiration term for  
316 mesozooplankton were reduced compared to model versions where no jellyfish are present (Table 5). Respiration  
317 is reduced in place of mortality for mesozooplankton as their mortality term had already been reduced to zero to  
318 account for predation by macrozooplankton (Le Quéré et al., 2016). The jellyfish PFT is also a significant grazer  
319 of protozooplankton, however, following the adjustment of protozooplankton grazing on picophytoplankton to



320 account for changes to the growth rate formulation and the low sensitivity of protozooplankton to jellyfish  
 321 mortality (Fig. 4) additional changes to protozooplankton parameters were found to be unnecessary.

**Table 5.** Changes to non-jellyfish PFT parameters across the PlankTOM simulations. PlankTOM10<sup>L-Q16</sup> is the latest published version of PlankTOM with 10 PFTs (Le Quéré et al., 2016), while PlankTOM10 is the simulation from this study.

Parameters	PlankTOM10 <sup>L-Q16</sup>	PlankTOM10	PlankTOM10.5	PlankTOM11
MAC mortality	0.020	0.012	0.005	0.005
MES respiration	0.014	0.014	0.001	0.001

322

### 323 2.1.7 Model Simulations

324

325 The PlankTOM11 simulations are run from 1920 to 2015, forced by meteorological data including daily wind  
 326 stress, cloud cover, precipitation and freshwater riverine input from NCEP/NCAR reanalysed fields (Kalnay et  
 327 al., 1996). The simulations start with a 28-year spin for 1920-1948 where the meteorological conditions for year  
 328 1980 are used, looping over a single year. Year 1980 is used as a typical average year, as it has no strong El  
 329 Nino/La Nina, as in Le Quéré et al. (2010). Furthermore, because of the greater availability of weather data  
 330 (including by satellite) in 1980 compared to 1948, the dynamical fields are generally more representative of small-  
 331 scale structures than the earlier years. There is a small shock to the system at the start of meteorological forcing,  
 332 but this stabilises within a few years and decades before the model output is used for analysis. Tests of different  
 333 spin-up years were carried out in Le Quéré et al. (2010), including both 1948 and 1980, with little impact on trends  
 334 generally. The spin up is followed by interannually varying forcing for actual years from 1948-2015. All analysis  
 335 is carried out on the average of the last 31-year period of 1985-2015. PlankTOM11 is initialised with observations  
 336 of dissolved inorganic carbon (DIC) and alkalinity (Key et al., 2004) after removing the anthropogenic component  
 337 for DIC (Le Quéré et al., 2010), NO<sub>3</sub>, PO<sub>4</sub>, SiO<sub>3</sub>, O<sub>2</sub>, temperature and salinity from the World Ocean Atlas  
 338 (Antonov et al., 2010).

339 Two further model simulations were carried out in order to better understand the effect of adding the jellyfish  
 340 PFT. The first simulation sets the jellyfish growth rate to 0, so that it replicates the model set up with 10 PFTs in  
 341 Le Quéré et al. (2016), here called PlankTOM10<sup>L-Q16</sup>, but it includes the updated growth formulation (Sect. 2.1.1)  
 342 and additional tuning (Sect. 2.1.5). The simulation is labelled 'PlankTOM10' in the figures. This simulation is  
 343 otherwise identical to PlankTOM11 except for the mortality term for macrozooplankton and the respiration term  
 344 for mesozooplankton, which were initially returned to PlankTOM10<sup>L-Q16</sup> values, to account for the lack of  
 345 predation by jellyfish. Macrozooplankton mortality was then tuned down from the PlankTOM10<sup>L-Q16</sup> value, from  
 346 0.02 to 0.012, to account for the change to the growth calculation (Table 5). The second additional simulation is  
 347 carried out to test the addition of an 11<sup>th</sup> PFT in comparison to the addition of jellyfish as the 11<sup>th</sup> PFT. This is  
 348 done by parameterising the jellyfish PFT identically to the macrozooplankton PFT in PlankTOM11, so that there  
 349 are 11 PFTs active, with two identical macrozooplankton. This simulation is called PlankTOM10.5. [The two](#)

350 [macrozooplankton in PlankTOM10.5 have mutual predation, where they prey on each other, while the](#)  
351 [macrozooplankton in PlankTOM10 have no preference for themselves. Subsequently, macrozooplankton](#)  
352 [mortality in PlankTOM10.5 is kept the same as PlankTOM11 \(Table 5\) to account for the mutual predation.](#)  
353 Otherwise, these simulations were identical to PlankTOM11.

354

## 355 2.2 JELLYFISH BIOMASS OBSERVATIONS

356

357 MARine Ecosystem biomass DATA (MAREDAT) is a database of global ocean plankton abundance and biomass,  
358 harmonised to common units and is open source available online (Buitenhuis et al., 2013b). The MAREDAT  
359 database is designed to be used for the validation of global ocean biogeochemical models. MAREDAT contains  
360 global quantitative observations of jellyfish abundance and biomass as part of the generic macrozooplankton  
361 group (Moriarty et al., 2013). The jellyfish sub-set of data has not been analysed independently yet.

362 For this study, all MAREDAT records under the group Cnidaria medusae ('true' jellyfish) were extracted from  
363 the macrozooplankton group (Moriarty et al., 2013) and examined. The taxonomic level within the database varies  
364 from phylum down to species. The data covers the period from August 1930 to August 2008 and contains  
365 abundance (individuals/m<sup>3</sup>, n=107,156) and carbon biomass ( $\mu\text{g}$  carbon L<sup>-1</sup>, n=3,406). The carbon biomass data  
366 are used over the abundance data despite the fewer data available, as they can be directly compared to  
367 PlankTOM11 results. Carbon biomass is calculated from wet weight/dry weight conversion factors for species  
368 where data records are sufficient (Moriarty et al., 2013). The data were collected at depth ranging from 0 to 2442m.  
369 The majority of the data (97%) were collected in the top 200m with an average depth of 44m ( $\pm$  32m). Data from  
370 the top 200m are included in the analysis. The original un-gridded biomass data were binned into 1°x1° degree  
371 boxes at monthly resolution, as in Moriarty et al. (2013), reducing the number of gridded biomass data points to  
372 849.

373 In MAREDAT, jellyfish biomass data are only present in the Northern Hemisphere, which is likely to skew the  
374 data. Another caveat to the data is that a substantially smaller frequency of zeros is reported for biomass than for  
375 abundance. Under-reporting of zero values will increase the average, regardless of the averaging method used.  
376 Biomass observations from other global studies (Bar-On et al., 2018; Lucas et al., 2014; Luo et al., 2020) are used  
377 conjunctly with the global jellyfish biomass calculated here because of the poor spatial coverage.

378 To compare to the other PFTs within the MAREDAT database, global jellyfish biomass was calculated according  
379 to the methods in Buitenhuis et al. (2013b). Buitenhuis et al. (2013b) calculate a biomass range, using the median  
380 as the minimum and the arithmetic mean (AM) as the maximum. The jellyfish zooplankton biomass range in  
381 MAREDAT was calculated as 0.46 – 3.11 PgC, with the median jellyfish biomass almost as high as the  
382 microzooplankton and higher than meso- and macrozooplankton (Buitenhuis et al., 2013b). The jellyfish biomass  
383 range calculated here is used to validate the new jellyfish component in the PlankTOM11 model.

## 384 3 RESULTS

### 385 3.1 JELLYFISH BIOMASS

386

387 The global jellyfish biomass estimated by various studies gives a range of results: 0.1 PgC (Bar-On et al., 2018),  
388  $0.32 \pm 0.49$  PgC (Lucas et al., 2014),  $0.29 \pm 0.56$  PgC (Luo et al., 2020, updated from Lucas et al.) and  $0.46 -$   
389  $3.11$  PgC calculated in this study (Sect. 2.2). Jellyfish biomass in PlankTOM11 is within the range but towards  
390 the lower end of observations at 0.13 PgC, with jellyfish accounting for 16% of the total zooplankton biomass  
391 (Table 6). When the modelled biomass was tuned to match the higher observed biomass by adjusting the mortality  
392 rate, jellyfish dominate the entire ecosystem significantly reducing levels of the other zooplankton and increasing  
393 chlorophyll above observations for the Northern and Southern Hemispheres (Fig. 4 and Fig. 5).

394 PlankTOM11 generally replicates the patterns of jellyfish biomass with observations. High biomass occurs at  
395 around 50-60°N across the oceans, with the highest biomass in the North Pacific. PlankTOM11 also replicates  
396 low biomass in the Indian Ocean, and the eastern half of the tropical Pacific shows higher biomass than other  
397 open ocean areas in agreement with patterns in observations (Fig. 6; Lucas et al., 2014; Luo et al., 2020). However,  
398 PlankTOM11 underestimates the high jellyfish biomass in the tropical Pacific (Fig. 6). Most of the data informing  
399 the jellyfish parameters is from temperate species, so the model will better represent higher latitudes than lower  
400 latitudes. This is likely responsible for some of the underestimation of biomass in this region. The competition of  
401 jellyfish with macrozooplankton also plays a role (see Sect. 3.3 for further discussion). The lack of biomass  
402 observations around 40°S makes it difficult to determine if the peak in jellyfish biomass in PlankTOM11 at this  
403 latitude is representative of reality. The maximum biomass in the southern hemisphere is mostly around coastal  
404 areas i.e. South America and southern Australia (Fig. 6). This is expected from reports and papers on jellyfish in  
405 these areas (Condon et al., 2013; Purcell et al., 2007 and references therein). A prevalence of jellyfish in coastal  
406 areas is apparent (Fig. 6), in line with observations (Lucas et al., 2014; Luo et al., 2020), even without any specific  
407 coastal advantages for jellyfish in the model (see macrozooplankton in Le Quéré et al., 2016).  
408 However, PlankTOM11 underestimates the range of observations in the top 200m (Fig. 6). PlankTOM11  
409 overestimates the minimum values and underestimates the maximum values. However, part of this discrepancy  
410 may be due to under-sampling in the observations. A key caveat in jellyfish data is that the data is not uniformly  
411 distributed spatially or temporally and not proportionally distributed between various biomes of the ocean, with  
412 collection efforts skewed to coastal regions and the Northern Hemisphere (MAREDAT; Lilley et al., 2011; Lucas  
413 et al., 2014; Luo et al., 2020). This sampling bias and sampling methods also tend to favour larger, less delicate  
414 species, which are often scyphomedusae with a meroplanktonic life cycle.

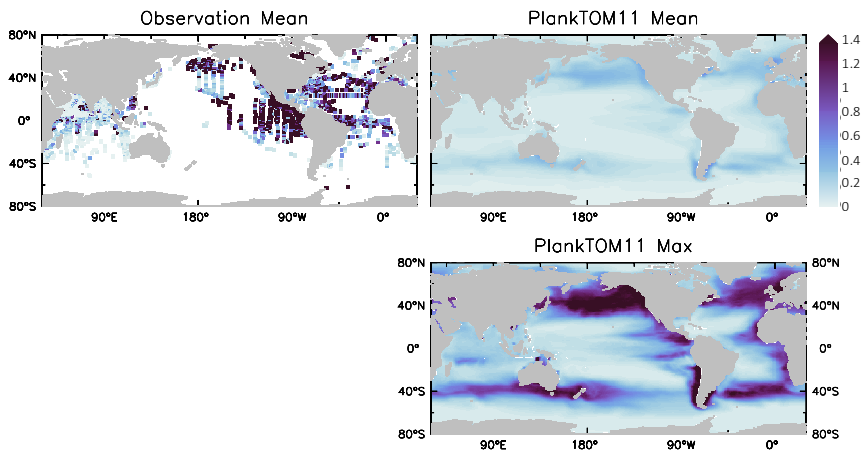
415 Jellyfish are characterised by their bloom and bust dynamic, resulting in patchy and ephemeral biomass. The  
416 mean:max biomass ratio of observations (MAREDAT) was compared to the same ratio for PlankTOM11 to assess  
417 the replication of this characteristic. The observations give a wide range of ratios depending on the type of mean  
418 used. The PlankTOM11 ratio falls within this range, but towards the lower end (Table 7). PlankTOM11 replicates  
419 some of the patchy and ephemeral biomass of jellyfish.

420 Jellyfish biomass in MAREDAT has poor global spatial coverage. The region around the coast of Alaska has the  
421 highest density of observations and is used here to evaluate the mean, range and seasonality of the carbon biomass  
422 of jellyfish as represented in PlankTOM11. The gridded jellyfish observations from Luo et al., (2020; see Fig. 6)

**Table 6.** Global mean values for rates and biomass from observations and the PlankTOM11 and PlankTOM10 models averaged over 1985–2015. In parenthesis is the percentage share of the plankton type of the total phytoplankton or zooplankton biomass. The percentage share of mixed-phytoplankton is not included, as there are no mixed-phytoplankton observations, therefore, the phytoplankton percentages are of total phytoplankton minus mixed-phytoplankton. References for observations are given in Appendix Table A5.

	PlankTOM11	PlankTOM10	Observations
<b>Rates</b>			
Primary production (PgC y <sup>-1</sup> )	41.6	43.4	51-65
Export production at 100m (PgC y <sup>-1</sup> )	7.1	7.0	5-13
CaCO <sub>3</sub> export at 100m (PgC y <sup>-1</sup> )	1.3	1.2	0.6-1.1
N <sub>2</sub> fixation (TgN y <sup>-1</sup> )	97.2	95.9	60-200
<b>Phytoplankton biomass 0-200m (PgC)</b>			
N <sub>2</sub> -fixers	0.065 (8%)	0.075 (10%)	0.008-0.12 (2-8%)
Picophytoplankton	0.141 (17%)	0.153 (20%)	0.28-0.52 (35-68%)
Coccolithophores	0.248 (30%)	0.212 (27%)	0.001-0.032 (0.2-2%)
Mixed-phytoplankton	0.263	0.268	-
Phaeocystis	0.177 (22%)	0.170 (22%)	0.11-0.69 (27-46%)
Diatoms	0.183 (22%)	0.167 (21%)	0.013-0.75 (3-50%)
Total phytoplankton biomass	1.077	1.046	0.412 – 2.112
<b>Heterotrophs biomass 0-200m (PgC)</b>			
Bacteria	0.041	0.046	0.25-0.26
Protozooplankton	0.295 (36%)	0.330 (32.7%)	0.10-0.37 (27-31%)
Mesozooplankton	0.193 (23%)	0.218 (21.6%)	0.21-0.34 (25-66%)
Macrozooplankton	0.205 (25%)	0.460 (45.6%)	0.01-0.64 (3-47%)
Jellyfish zooplankton	0.129 (16%)	-	0.10-3.11
Total zooplankton biomass	0.823	1.008	0.42 – 4.46

423 are available as a mean over time and depth, so cannot be used to evaluate range or seasonality. Spatially, the

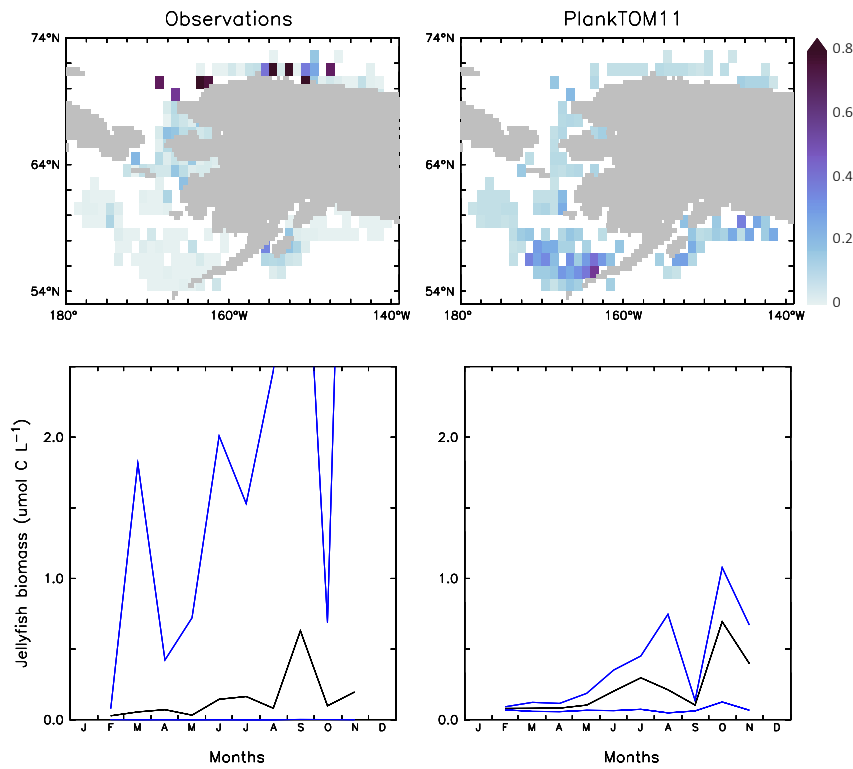


424 *Figure 6. Jellyfish carbon biomass ( $\mu\text{mol C L}^{-1}$ ) in PlankTOM11 and in observations from the Jellyfish Database Initiative (Luo*  
 425 *et al., 2020). PlankTOM11 results (left) are the mean and maximum biomass from monthly climatologies. Observations (right)*  
 426 *are the mean biomass, areas with no observations are in white. Observations are on a  $1 \times 1^\circ$  grid and are plotted using a*  
 427 *three-cell averaging filler for visual clarity. All data is for 0-200m. The gridded observation data is only available as a mean*  
 428 *over time and depth (Luo et al., 2020). Due to the patchy nature of the observations in depth and time, the mean may be*  
 429 *skewed high or low, while the model is sampled across the full time and depth.*

430 observations peak around the north coast of Alaska while PlankTOM11 peaks around the south coast (Fig. 7).  
 431 This difference is likely due to the lack of small-scale physical processes in the model due to the relatively coarse  
 432 model resolution. PlankTOM11 reproduces the observed mean jellyfish biomass around the coast of Alaska ( $0.16$   
 433 compared to  $0.13 \mu\text{mol C L}^{-1}$ ), but it underestimates the maximum and spread of the observations (Table 8). The  
 434 spatial patchiness is somewhat replicated in PlankTOM11, although with a smaller variation (Fig. 7).  
 435 PlankTOM11 replicates the mean seasonal shape and biomass of jellyfish with a small peak over the summer  
 436 followed by a large peak in September in the observations and in October in PlankTOM11 (Fig. 7). Overall,  
 437 PlankTOM11 replicates the mean but underestimates the maximum biomass and temporal patchiness of the  
 438 observations (Fig. 7 and Table 8).

**Table 7.** Jellyfish biomass globally from observations (MAREDAT) and PlankTOM11. Three types of mean are given for the observations; Med is the median, AM is the arithmetic mean and GM is the geometric mean. The ratios are all scaled to mean = 1. All units are  $\mu\text{g C L}^{-1}$ .

		Mean	Max	Ratio
Observations	AM	3.61	156.0	1 : 43
	GM	0.95	156.0	1 : 165
	Med	0.29	156.0	1 : 538
PlankTOM11	AM	1.18	98.9	1 : 84



439

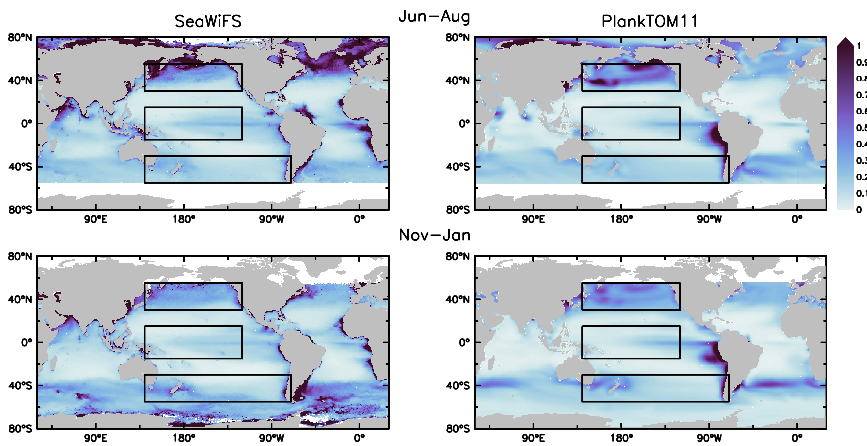
440 *Figure 7. Carbon biomass of jellyfish ( $\mu\text{mol C L}^{-1}$ ) from MAREDAT observations (left) and PlankTOM11 (right) for the coast of*  
 441 *Alaska (the region with the highest density of observations). The top panels show the mean jellyfish biomass and the bottom*  
 442 *panels show the seasonal jellyfish biomass, with the monthly mean in black and the monthly minimum and maximum in blue.*  
 443 *Observations and PlankTOM11 results are for 0-150m, as the depth range where >90% of the observations occur. No*  
 444 *observations were available for January or December.*

445

### 446 3.2 ECOSYSTEM PROPERTIES OF PLANKTOM11

447

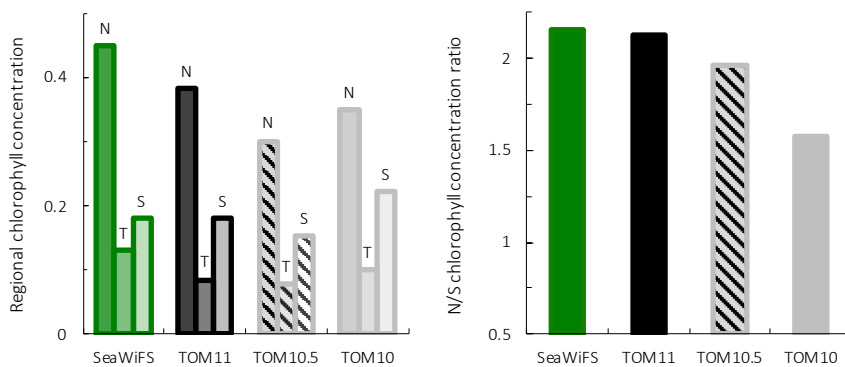
448 PlankTOM11 reproduces the main characteristics of surface chlorophyll observations, with high chlorophyll  
 449 concentration in the high latitudes, low concentration in the subtropics and elevated concentrations around the  
 450 equator (Fig. 8). PlankTOM11 also reproduces higher chlorophyll concentrations in the Northern Pacific than the  
 451 Southern (Fig. 9), and higher concentrations in the southern Atlantic than the southern Pacific Ocean (Fig. 8).  
 452 Overall the model underestimates chlorophyll concentrations, as is standard with models of this type (Le Quéré  
 453 et al., 2016) particularly in the central and northern Atlantic. PlankTOM11 also captures the seasonality of  
 454 chlorophyll, with concentrations increasing in summer compared to the winter for each hemisphere (Fig. 8).



455

456 *Figure 8. Surface chlorophyll ( $\mu\text{g chl L}^{-1}$ ) averaged for June to August (top) and November to January (bottom). Panels show*  
 457 *observations from SeaWIFS (left) satellite and results from PlankTOM11 (right). Observations and model are averaged for*  
 458 *1997-2006. The black boxes show the Pacific north, tropic and south regions used in Fig. 4 and Fig. 9.*

459



460

461 *Figure 9. Surface chlorophyll for observations from SeaWIFS satellite, PlankTOM11, PlankTOM10.5 and PlankTOM10.*  
 462 *Regional chlorophyll concentration in  $\mu\text{g chl L}^{-1}$  (right) for the north (N), tropic (T) and south (S) Pacific Ocean regions shown*  
 463 *in Fig. 8 and the N/S chlorophyll concentration ratio (left). Observations and model are averaged for 1997-2006.*

464

465 To assess the effect of adding jellyfish to PlankTOM, two additional simulations were conducted: PlankTOM10  
 466 where jellyfish growth is set to zero and PlankTOM10.5 where all jellyfish parameters are set equal to  
 467 macrozooplankton parameters (Sect. 2.1.6). The two simulations show similar spatial patterns of surface  
 468 chlorophyll to PlankTOM11, but different concentration levels. PlankTOM11 closely replicates the chlorophyll  
 469 ratio between the north and south Pacific with a ratio of 2.12, compared to the observed ratio of 2.16 (Fig. 9).

470 PlankTOM10 and PlankTOM10.5 underestimate the observed ratio with ratios of 1.57 and 1.96 respectively (Fig.  
471 9). Adding an 11<sup>th</sup> PFT improves the chlorophyll ratio, however, the regional chlorophyll concentrations for  
472 PlankTOM10.5 are a poorer match to the observations than PlankTOM11, especially in the north (Fig. 9).  
473 PlankTOM10 overestimates the observed chlorophyll concentration in the south (0.22 and 0.18 respectively; Fig.  
474 9). All three simulations underestimate chlorophyll concentration in the tropics compared to observations (Fig.  
475 9). The north/south chlorophyll ratio metric was developed by Le Quéré et al. (2016) as a simple method to  
476 quantify model performance for emergent properties, focussing on the Pacific Ocean as the area where this ratio  
477 is most pronounced in the observations. These simulations further support the suggestion by Le Quéré et al. (2016)  
478 that the observed distribution of chlorophyll in the north and south is a consequence of trophic balances between  
479 the PFTs and improves with increasing plankton complexity.

480 PlankTOM11 underestimates primary production by 10 PgC y<sup>-1</sup>, which is similar to the underestimation in  
481 PlankTOM10<sup>LQ16</sup> of 9 PgC y<sup>-1</sup>. As suggested by Le Quéré et al. (2016) this may be due to the model only  
482 representing highly active bacteria, which is unchanged between the model versions, while observed biomass is  
483 also from low activity bacteria and ghost cells. Export production and N<sub>2</sub> fixation are within the observational  
484 range, and CaCO<sub>3</sub> export is slightly overestimated (Table 6).

485 In PlankTOM11 each PFT shows unique spatial distribution in carbon biomass (Fig. 5). The total biomass of  
486 phytoplankton is within the range of observations, but the partitioning of this biomass between phytoplankton  
487 types differs from observations (Table 6). PlankTOM11 is dominated by mixed-phytoplankton and  
488 coccolithophores, together making up 47% of the total phytoplankton biomass. Diatoms and *Phaeocystis* are the  
489 next most abundant and fall within the observed range, followed by picophytoplankton with around half the  
490 observed biomass (Table 6). The observations are dominated by picophytoplankton, followed by *Phaeocystis* and  
491 Diatoms (Table 6). The modelled mixed-phytoplankton is likely taking up the ecosystem niche of  
492 picophytoplankton. Coccolithophores are overestimated by a factor of 10 and may also be filling the ecosystem  
493 niche of picophytoplankton in the model (Table 6). The phytoplankton community composition changed from  
494 PlankTOM10<sup>LQ16</sup> to PlankTOM11, with some phytoplankton types moving closer to observations and some  
495 moving further away. For example, for N<sub>2</sub>-fixers PlankTOM11 is in line with the upper end of observations at  
496 8%, while PlankTOM10 and PlankTOM10<sup>LQ16</sup> overestimate N<sub>2</sub>-fixers (10% and 11% respectively). For  
497 picophytoplankton, PlankTOM10<sup>LQ16</sup> is within the range of observations at 38%, while PlankTOM11 and  
498 PlankTOM10 underestimate the community share of picophytoplankton (17% and 20% respectively). For  
499 *Phaeocystis*, all three simulations underestimate the community share, but PlankTOM11 and PlankTOM10 (both  
500 22%) are closer to the lower end of observations (27%) than PlankTOM10<sup>LQ16</sup> (15%; Table 6; Le Quéré et al,  
501 2016). Overall, the difference between PlankTOM10<sup>LQ16</sup> and PlankTOM11 is greater than the difference between  
502 PlankTOM10 and PlankTOM11, suggesting that the change to growth of PFT's had a larger effect on  
503 phytoplankton community composition than the addition of jellyfish. This is expected, as the growth change  
504 directly effects each PFT and model results are sensitive to PFT growth rates (Buitenhuis et al., 2006, 2010).  
505 Jellyfish affect phytoplankton community composition, but the effect is small.

506

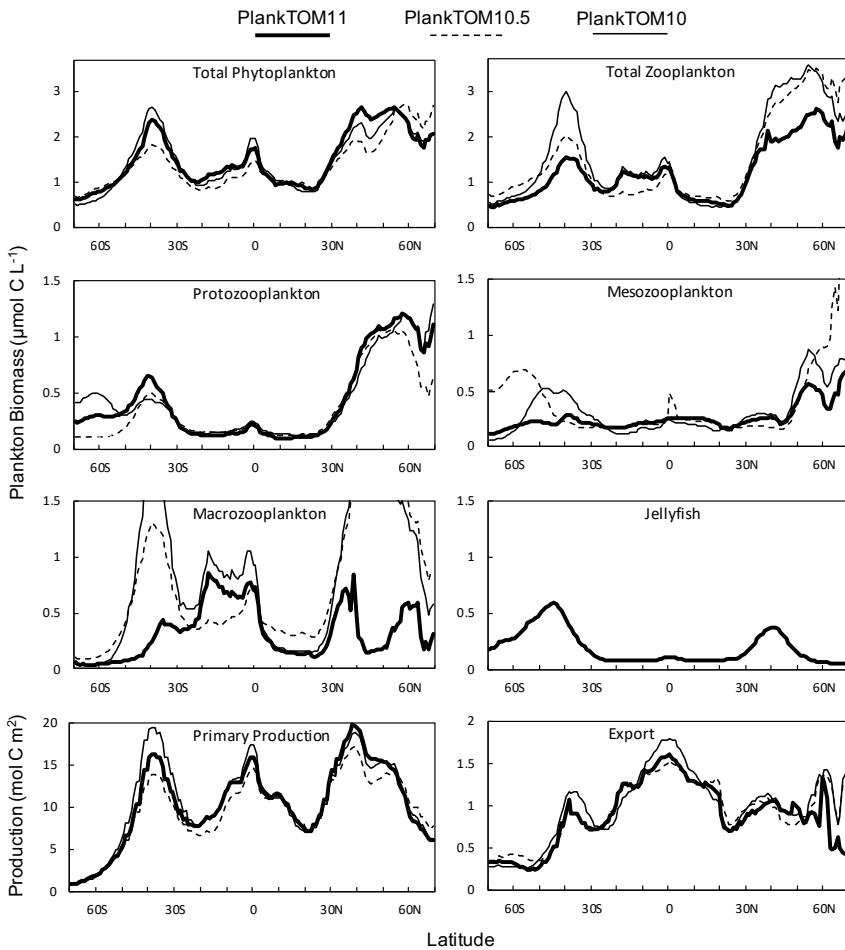


### 507 3.3 ROLE OF JELLYFISH IN THE PLANKTON ECOSYSTEM

508

509 Macrozooplankton exhibit the largest change in biomass between the three simulations, followed by  
510 mesozooplankton (Fig. 10). This is despite the higher preference of jellyfish grazing on mesozooplankton (ratio  
511 of 10) than on macrozooplankton (ratio of 5; Table 3). The central competition for resources between jellyfish  
512 and macrozooplankton is that they both preferentially graze on mesozooplankton, then on protozooplankton,  
513 although macrozooplankton have a lower preference ratio for zooplankton than jellyfish, as more of their diet is  
514 made up by phytoplankton (Table 3). In simple terms this means that for two equally sized populations of jellyfish  
515 and macrozooplankton, jellyfish would consume more meso- and protozooplankton than would be consumed by  
516 macrozooplankton. However, predator biomass, prey biomass and the temperature dependence of grazing interact  
517 to affect the rate of consumption (Eq. 5). The greatest difference in PFT biomass, especially macrozooplankton  
518 biomass, between simulations occurs in latitudes higher than 30° where jellyfish biomass is highest (Fig. 10). In  
519 the tropics, jellyfish have a low impact on the ecosystem due to their low biomass in this region (Fig. 6 and Fig.  
520 10).

521 The seasonality of the PFTs in each simulation is shown in Fig. 11 for 30-70° north and south, as the regions with  
522 the greatest differences between simulations (Fig. 10). In PlankTOM10 macrozooplankton represent the highest  
523 trophic level. The addition of another PFT at the same or at a higher trophic level (PlankTOM10.5 and  
524 PlankTOM11 respectively) reduces the biomass of the macrozooplankton, through a combination of competition  
525 and low-level predation (Fig. 10 and Fig. 11). For PlankTOM10.5 results, macrozooplankton is summed with the  
526 11<sup>th</sup> PFT (identical to macrozooplankton in this simulation). The addition of this 11<sup>th</sup> PFT at the same trophic  
527 level reduces the biomass of the macrozooplankton (Fig. 10 and Fig. 11), despite the macrozooplankton mortality  
528 being reduced from PlankTOM10 to PlankTOM10.5 (Table 5) which would be expected to increase  
529 macrozooplankton biomass. However, the low level of mutual predation between the two macrozooplankton PFTs  
530 slightly reduces their overall biomass. This reduction in biomass mostly occurs during the autumn  
531 macrozooplankton bloom, where the peak is reduced from PlankTOM10 to PlankTOM10.5, while the winter –  
532 spring biomass is similar across the two simulations (Fig. 11). The drop in mesozooplankton respiration from  
533 PlankTOM10 to PlankTOM10.5 (Table 5) lowers the rate of respiration, especially at lower temperatures. This  
534 likely accounts for the increase in PlankTOM10.5 mesozooplankton biomass at higher latitudes (Fig. 10). The  
535 addition of jellyfish changes the zooplankton with the highest biomass from macrozooplankton to  
536 protozooplankton and reduces the biomass of mesozooplankton, in both the north and south (Fig. 11). However,  
537 the impact on the biomass of mesozooplankton and protozooplankton is small, despite mesozooplankton being  
538 the preferential prey of jellyfish, followed by protozooplankton. The small impact of jellyfish on mesozooplankton  
539 and protozooplankton biomass may be due to trophic cascade effects where jellyfish reduce the biomass of  
540 macrozooplankton, which reduces the predation pressure of macrozooplankton on meso- and protozooplankton,  
541 whilst jellyfish simultaneously provide an additional predation pressure on meso- and protozooplankton. The  
542 decrease in predation by macrozooplankton may be compensated for by the increase in predation by jellyfish,  
543 resulting in only a small change to the overall biomass of mesozooplankton and protozooplankton.



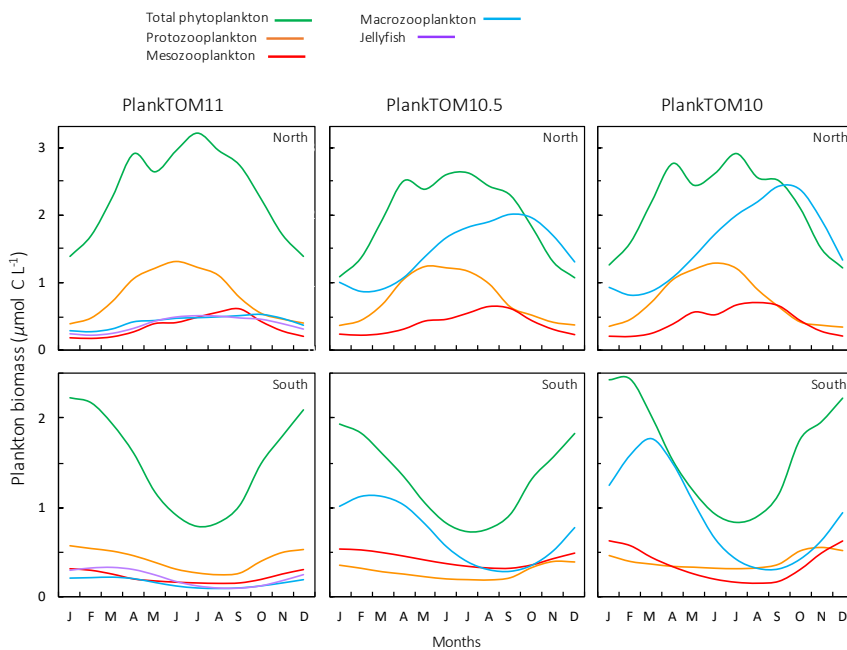
544

545 **Figure 10.** Zonal mean distribution for the PlankTOM11, PlankTOM10.5 and PlankTOM10 simulations. All plankton biomass  
 546 data are for the surface box (0-10m). For PlankTOM10.5 the MAC PFT has been summed with the 11<sup>th</sup> PFT that duplicates  
 547 MAC. The bottom panels are the zonal mean distribution of primary production, integrated over the top 100m, and export  
 548 production at 100m. All data are averaged for 1985-2015.

549 In PlankTOM11 there is a clear distinction between the biomass in the north and south, with higher biomass for  
 550 each PFT in the north compared to the south (Fig. 10 and Fig. 11). Plankton types have higher concentrations in  
 551 the respective hemisphere's summer, and a double peak in phytoplankton in the north (Fig. 11). PlankTOM10  
 552 also has a higher biomass of each PFT in the north compared to the south, but the difference is smaller than that  
 553 in PlankTOM11 (Fig. 10 and Fig. 11). The key difference between the two models is the biomass of  
 554 macrozooplankton. In PlankTOM10 macrozooplankton are the dominant zooplankton, especially in late summer  
 555 and autumn where their biomass matches and even exceeds the biomass of phytoplankton in the region (Fig. 11).  
 556 In PlankTOM11 neither macrozooplankton, nor any other zooplankton, come close to matching the biomass of

557 phytoplankton. The largest direct influence of jellyfish in these regions is its role in controlling macrozooplankton  
 558 biomass, through competition for prey resources, particularly mesozooplankton and protozooplankton, and  
 559 through the predation of jellyfish on macrozooplankton.

560 In PlankTOM11 in the north, phytoplankton display a double peak in seasonal biomass, with a smaller peak in  
 561 April of  $2.9 \mu\text{mol C L}^{-1}$ , followed by a larger peak in July of  $3.2 \mu\text{mol C L}^{-1}$  (Fig. 11). The addition of jellyfish  
 562 amplifies these peaks from PlankTOM10 and PlankTOM10.5 (Fig. 11) and from PlankTOM10 (Le Quéré et al.,  
 563 2016). Observations (MAREDAT) show two peaks in phytoplankton biomass although the peaks are offset in  
 564 timing from all three PlankTOM simulations. The amplitude of the full seasonal cycle in observations is  $0.78 -$   
 565  $2.67 \mu\text{mol C/L}$  (median – mean) with all three PlankTOM simulations falling well within this range (Table A6).  
 566 Removing the winter months, where there is less variability, gives a non-winter observational amplitude of  $0.7 -$   
 567  $2.12 \mu\text{mol C/L}$ . PlankTOM11 is the highest, with a non-winter amplitude of  $0.97 \mu\text{mol C/L}$ , with the other two  
 568 simulations lower at  $0.8 \mu\text{mol C/L}$  (PlankTOM10.5) and  $0.81 \mu\text{mol C/L}$  (PlankTOM10; Table A6).  
 569 PlankTOM10<sup>L-Q16</sup> has a lower seasonal amplitude than PlankTOM11, although a slighter higher non-winter  
 570 amplitude by  $0.05 \mu\text{mol C/L}$  (Table A6). The changes to phytoplankton seasonal biomass are not evenly  
 571 distributed across the PFT's, with coccolithophores and Phaeocystis exhibiting the largest changes (Fig. A1).



572

573 **Figure 11.** Seasonal surface carbon biomass ( $\mu\text{mol C L}^{-1}$ ) of total phytoplankton PFTs, protozooplankton, mesozooplankton,  
 574 macrozooplankton and jellyfish. For PlankTOM10.5 the MAC PFT has been summed with the 11<sup>th</sup> PFT that duplicates MAC.  
 575 Panels shown PFT biomass for PlankTOM11 (left), PlankTOM10.5 (middle) and PlankTOM10 (right), for two regions; the north  
 576  $30^{\circ}\text{N} - 70^{\circ}\text{N}$  (top) and the south  $30^{\circ}\text{S} - 70^{\circ}\text{S}$  (bottom) across all longitudes. All data are averaged for 1985-2015.

577 Primary production follows a similar pattern to total phytoplankton biomass across the three simulations, with  
578 higher biomass across more latitudes in the north compared to the south, although primary production differs from  
579 phytoplankton at the equator where it reaches a similar magnitude peak as in the south (Fig. 10). Export production  
580 has a markedly different zonal mean distribution across latitudes than PFT biomass and primary production, with  
581 the highest production in the tropics for all three simulations. The large variation in zooplankton biomass in the  
582 north and south between the three simulations is not reflected in export production, as would be expected (Fig.  
583 10). Around 40°S and 0° PlankTOM10 primary production peaks and is the highest of the three simulations. This  
584 is reflected in PlankTOM10 export peaking at the same latitudes. Around 30-55°N PlankTOM11 primary  
585 production peaks and is the highest of the three simulations, but this is not reflected in PlankTOM11 export  
586 peaking over the same latitudes (Fig. 10). Due to the lower total zooplankton biomass in PlankTOM11 compared  
587 to the other two simulations, mostly due to the reduced macrozooplankton, driven by the peak in jellyfish biomass.  
588 primary production peaks as there is reduced grazing on phytoplankton, but due to lower zooplankton biomass  
589 and therefore less zooplankton egestion, excretion and mortality there is less production of POC<sub>L</sub>.

590 Globally primary production is higher in PlankTOM10, than in PlankTOM11, but export is slightly lower, as are  
591 POC<sub>S</sub> and POC<sub>L</sub> (Table 6; Fig. A2), indicating that more of the carbon is retained and circulated in the plankton  
592 ecosystem in PlankTOM10 than in PlankTOM11. This is not just due to an additional top PFT, as in  
593 PlankTOM10.5, primary production and export are the lowest (Table 6; Fig. A2). However, as mentioned  
594 previously, the changes to export are smaller than expected given the large changes to zooplankton biomass and  
595 ecosystem structure. This is likely due to a bottle neck effect in the model structure, where, for example, mortality  
596 from three zooplankton PFTs, enters a single pool (Fig. 1b).

597

## 598 4 DISCUSSION

599

600 Model results suggest high competition between macrozooplankton (crustaceans) and jellyfish, with a key role of  
601 jellyfish being its control on macrozooplankton biomass, which via trophic cascades influences the rest of the  
602 plankton ecosystem, [across plankton community structure, spatiotemporal dynamics, and biomass](#). The growth  
603 rate of jellyfish is higher than that of macrozooplankton for the majority of the ocean (where the temperature is  
604 less than ~25°C) but the mortality of jellyfish is also significantly higher than macrozooplankton, again for the  
605 majority of the ocean. The combination of high growth and mortality means that jellyfish have a high turnover  
606 rate in temperate waters. In situations where jellyfish mortality is reduced (but still higher than macrozooplankton  
607 mortality), jellyfish outcompete macrozooplankton for grazing. Below 20°C jellyfish and macrozooplankton  
608 respiration is almost the same, so will have minimal influence on their relative biomass. Biomass is not linearly  
609 related to the growth, respiration and mortality rates, with biomass also dependent on prey availability, total PFT  
610 biomass and other variables. Because jellyfish also prey directly on macrozooplankton, the biomass of  
611 macrozooplankton can rapidly decrease in a positive feedback mechanism. Within oligotrophic regions both  
612 jellyfish and macrozooplankton biomass is low, as expected due to limited nutrients limiting phytoplankton  
613 growth in these regions. Around equatorial upwelling regions, macrozooplankton outcompete jellyfish.

614 Macrozooplankton also outcompete jellyfish in many coastal areas including around northern Eurasia because  
615 they have a built-in coastal and under-ice advantage to represent enhanced recruitment in these environments  
616 which likely tips the balance in their favour (Le Quéré et al., 2016). Around 40°S and 40-50°N jellyfish mostly  
617 outcompete macrozooplankton, water temperature here is around 10-17°C which is a temperature where jellyfish  
618 growth is the most above macrozooplankton growth and macrozooplankton mortality nearing jellyfish mortality,  
619 which combined together favour jellyfish over macrozooplankton. This sensitivity of the composition of the  
620 zooplankton community to the mortality of jellyfish could help explain why jellyfish are seen as increasing  
621 globally. A reduction in jellyfish mortality during early life-stages i.e. through reduced predation on ephyrae and  
622 juveniles by fish (Duarte et al., 2013; Lucas et al., 2012), could quickly allow jellyfish to outcompete other  
623 zooplankton, especially macrozooplankton.

624 The high patchiness of jellyfish in the observations is partly but not fully captured in PlankTOM11 (Fig. 7 and  
625 Table 7). The reasons for limited patchiness include the model resolution of  $\sim 2^\circ \times 1^\circ$  which doesn't allow for the  
626 representation of small-scale physical mixing such as eddies and frontal regions, which have been shown to  
627 influence bloom formation (Benedetti-Cecchi et al., 2015; Graham et al., 2001). Physical processes are likely to  
628 be more responsible for jellyfish patchiness than behaviours, due to their simplistic locomotion. For example,  
629 many jellyfish blooms occur around fronts, upwelling regions, tidal and estuarine regions, and shelf-breaks where  
630 currents can aggregate and retain organisms (Graham et al., 2001). A few large individuals of the species  
631 *Rhizostoma octopus* (barrel jellyfish) have been found to have the capacity to actively swim counter current that  
632 could aim to orientate themselves with currents, with the potential to aid bloom formation and retention (Fossette  
633 et al., 2015). However, this active swimming behaviour is not representative across the group and would only  
634 move the jellyfish within an area less than the resolution of the model. Furthermore, there is currently insufficient  
635 data and an incomplete understanding of such swimming behaviours to include it in a global model.

636 The maximum biomass of jellyfish in PlankTOM11 is  $98.9 \mu\text{g C L}^{-1}$ , compared to the observed maximum biomass  
637 of  $156 \mu\text{g C L}^{-1}$  and the mean: max ratio is within the range of observations although towards the lower end (Table  
638 7). This demonstrates that even without replication of high patchiness, PlankTOM11 still achieved some  
639 ephemeral blooms where jellyfish achieved a high biomass.

640 A key limitation of the representation of jellyfish in the model is the exclusion of the full life cycle. Most jellyfish  
641 display metagenesis, alternating between a polyp phase that reproduces asexually and a medusa phase that  
642 reproduces sexually (Lucas and Dawson, 2014). PlankTOM11 currently only characterises the pelagic phase of  
643 the jellyfish life cycle, with parameters based on data from the medusae and ephyrae. The biomass of jellyfish is  
644 maximal during the pelagic medusa stage, as medusae are generally several orders of magnitude larger than polyps  
645 and one polyp can release multiple ephyrae into the water column (Lucas and Dawson, 2014). Although most  
646 hydromedusae persist in the plankton for short periods of time, larger scyphomedusae can live for 4-8 months and  
647 individuals in some populations can survive for more than a year by overwintering; something that may be  
648 facilitated by global climate change (Boero et al., 2016). Polyps develop from planula larvae within 5 weeks of  
649 settlement, and can persist far longer than medusae owing to their asexual mode of reproduction and the fact that  
650 they can encyst, which allows them to remain dormant until environmental conditions are favourable for budding  
651 (Lucas and Dawson, 2014). Unusually, mature medusae of *Turritopsis dohrnii* can revert back to the polyp stage

652 and repeat the life cycle, which effectively confers immortality (Martell et al., 2016). Our understanding of polyp  
653 ecology is almost entirely based on laboratory reared specimens of common, eurytolerant species, with the  
654 patterns observed being locale- and species-dependent. We know that temperature changes can trigger the budding  
655 of ephyrae by scyphopolyps, which may lead to an increase in the medusa population (Han and Uye, 2010; Lucas  
656 and Dawson, 2014), but the number of species whose polyps have been located and studied in situ is minuscule  
657 and so estimates of polyp abundance or biomass are impossible even to estimate.

658 Models that include the full jellyfish life cycle are still relatively new, and their focus has been locale- and species-  
659 dependant (e.g. Henschke et al., 2018; Schnedler-Meyer et al., 2018). The aim of this study was not to reproduce  
660 small-scale blooms, but rather to assess at the large and global scale the influence of jellyfish on the plankton  
661 ecosystem and biogeochemistry. We consider it enough to note that higher temperature within PlankTOM11  
662 increases the growth rate, which translates into increased biomass if there is sufficient food, thus providing a  
663 representation of an increasing medusa population. The inclusion of jellyfish life cycles into PlankTOM11 would  
664 introduce huge uncertainties due to the lack of clear in situ life cycle data and is beyond the scope of the exercise.

665 There is currently no coastal advantage for jellyfish included in the model, as there is for macrozooplankton,  
666 which have a coastal and under-ice advantage for increased recruitment (Le Quéré et al., 2016). Introducing a  
667 similar coastal advantage for jellyfish could introduce an element of life cycle benefits i.e. the increased  
668 recruitment and settlement of planula larvae onto hard substrate in coastal regions and also ephyrae released from  
669 nearshore systems may benefit from being in nearshore waters (restricted there by mobility and current-closure  
670 systems) in much the same way as for other neritic planktonic taxa (Lucas et al., 2012). Alternatively, a deep-  
671 water disadvantage could be introduced for jellyfish to introduce an element of their life cycle dependencies in  
672 that the polyps require benthic substrate for settlement and development into the next life stage and are dependent  
673 on plankton for food, which are more abundant in shallower coastal waters. Future work on PlankTOM11 could  
674 investigate the strengths and weaknesses of these two avenues (coastal advantage and deep-water disadvantage)  
675 for introducing a jellyfish lifecycle element.

676 Jellyfish in PlankTOM11 are parameterised using data largely from temperate species, because this is the majority  
677 of the data available. This may explain some of the prevalence of jellyfish in PlankTOM11 at mid- to high-  
678 latitudes and the lower biomass in the tropics. Experimental rate data for a wider range of jellyfish species from  
679 a wider range of latitudes is required to address this bias. Another limitation of jellyfish representation in the  
680 model is the lack of body size representation. Generally smaller individuals have greater biological activity, while  
681 larger individuals have greater biomass. Depending on the time of year and life history strategy the dominant  
682 source of biomass will shift between smaller and larger individuals. The size distribution of body mass in jellyfish  
683 is particularly wide compared to other PFTs (Table 1), so representing jellyfish activity by an average sized  
684 individual could well skew the results.

685 Trophic interactions explain the improvement of spatial chlorophyll with the introduction of jellyfish to the model  
686 (PlankTOM10 to PlankTOM10.5 to PlankTOM11), especially the North/South ratio. The three simulations have  
687 identical physical environments, with the influence of jellyfish as the only alteration, so any differences between  
688 the three can be attributed to the ecosystem structure. Jellyfish are the highest trophic level represented in  
689 PlankTOM11, with preference for meso-, followed by proto-, and then macrozooplankton. However, the largest

690 influence of jellyfish is on the macrozooplankton, because the grazing pressure on mesozooplankton from  
691 macrozooplankton is reduced, and the grazing on protozooplankton by macro- and mesozooplankton is reduced,  
692 while the grazing pressure from jellyfish on both meso- and protozooplankton is increased. The combined changes  
693 to macrozooplankton and jellyfish grazing pressure counteract to reduce the overall change in grazing pressure.  
694 The top down trophic cascade from jellyfish on the other zooplankton also changes some of the grazing pressures  
695 on the phytoplankton, which translates into regional and seasonal effects on chlorophyll. Jellyfish increase  
696 chlorophyll in the northern pacific and reduce it in the southern pacific, relative to PlankTOM10 (Fig. 9).  
697 Seasonally, in the global north jellyfish increase phytoplankton biomass most during the summer and in the global  
698 south jellyfish decrease phytoplankton biomass most during the summer, relative to PlankTOM10 (Fig. 11). In  
699 the north, most of this summer increase in phytoplankton comes from coccolithophores and *Phaeocystis*, while in  
700 the south most of the summer decrease comes from coccolithophores, picophytoplankton and mixed  
701 phytoplankton (Fig. A1).

702 The complexity of zooplankton has been increased, however, the complexity of particulate organic carbon has  
703 not, resulting in a bottleneck in carbon export. The low sensitivity of the modelled export to changes in  
704 zooplankton composition is likely due to the small number of particulate organic carbon pools. For example,  
705  $POC_L$  would export the same carbon particulate whether mesozooplankton, macrozooplankton or jellyfish  
706 dominate. There is variety built into the zooplankton contribution to  $POC_L$  as the amount entering is dependent  
707 on the grazing rate, growth, biomass etc. of each zooplankton, but it all becomes one type of particulate matter  
708 once it enters the pool.

709 The two pools of particulate organic carbon in PlankTOM11 are insufficient to represent the variety of particulate  
710 organic carbon generated by the increased variety of zooplankton as the model has been developed. The  
711 contribution of mortality to  $POC_L$  is orders of magnitude different between mesozooplankton and jellyfish  
712 carcasses. The composition of the carcasses is also very different, with the high water-content of jellyfish compared  
713 to other zooplankton, which effects the carcass sinking behaviour (Lebrato et al., 2013a). Mass deposition events  
714 of jellyfish carcasses (jelly-falls), at depths where the carbon is unlikely to be recycled back into surface waters at  
715 short to medium time scales, are known to contain significant amounts of carbon and can contain in excess of a  
716 magnitude more carbon than the annual carbon flux (Billett et al., 2006; Yamamoto et al., 2008). PlankTOM11  
717 likely substantially underestimates jellyfish contribution from mortality (Luo et al., 2020). Through rapidly  
718 sinking jelly-falls, jellyfish cause a large pulse in export (Lebrato et al., 2012, 2013a, 2013b), not yet accounted  
719 for in PlankTOM11. The global export in PlankTOM11 (7.11 PgC/y) is within global estimates of 5 - 12 PgC/y.  
720 The main reason for export being towards the lower end of observations is that the global primary production in  
721 PlankTOM11 is lower than the observed rate. Another potential explanation which may enhance the low export  
722 is that within the model jellyfish have a high turnover rate, due to their high growth, grazing and mortality rates,  
723 thus taking in a high proportion of carbon, but they are not then acting as a direct rapid source of sinking carbon  
724 through their mortality.

725 The contribution of egestion and excretion (see Fig. 1b and Fig. A2) to  $POC_L$  is also very different between  
726 mesozooplankton, macrozooplankton and jellyfish, most particularly that the main contribution from meso- and  
727 macrozooplankton is in the form of solid faecal pellets, while for jellyfish the main contribution is from mucus  
728 (Hansson and Norrman, 1995). The composition and sinking behaviour of faecal pellets and mucus will be

729 substantially different, with mucus sinking more slowly and more likely to act as a nucleus for enhanced  
730 aggregation with other particles, forming a large low-density mass (Condon et al., 2011; Pitt et al., 2009).

731 Work is currently underway on PlankTOM to increase the size partitioning of particulate organic carbon through  
732 introducing a size-resolving spectral model with a spectrum of particle size and size-dependent sinking velocity  
733 (Kriest and Oeschlies, 2008). This method has the advantage of improving the representation of particulate organic  
734 carbon production from all PFTs but is substantially more computer expensive. Another role of jellyfish may be  
735 that they act as significant vectors for carbon export, but with the current POC partitioning in PlankTOM11 this  
736 role has not been elucidated here. The potential influence of introducing increased size partitioning on carbon  
737 export could be significant, with peaks in jellyfish biomass being followed by a pulse in carbon export as there is  
738 rapid sinking of large carcasses (Lebrato et al., 2012; Luo et al., 2020).

739 Jellyfish have been included in a range of regional models, the majority are fisheries-based ecosystem models,  
740 namely ECOPATH and ECOPATH with ECOSIM (Pauly et al., 2009). These include regional models of the  
741 Northern Humboldt Current system (Chiaverano et al., 2018), the Benguela Upwelling System (Roux et al., 2013;  
742 Roux and Shannon, 2004; Shannon et al., 2009) and an end-to-end model of the Northern California Current  
743 system, based on ECOPATH (Ruzicka et al., 2012). Jellyfish have also been included in regional Nutrient  
744 Phytoplankton Zooplankton Detritus (NPZD) models, representing small-scale coastal temperate ecosystems with  
745 simple communities, for example, Schnedler-Meyer et al. (2018) and Ramirez-Romero et al. (2018). These models  
746 have provided valuable insight into jellyfish in the regions studied, but the focus on coastal ecosystems and either  
747 a top-down approach (ECOPATH) or highly simplified ecosystem (NPZD) limits their scope. [A recent paper has](#)  
748 [included jellyfish in a global ecosystem model, including multiple other zooplankton and fish types and provides](#)  
749 [a static representation of biomass \(Heneghan et al., 2020\). However, the model does not include phytoplankton,](#)  
750 [biogeochemistry \(outside of using carbon content to determine zooplankton functional groups\) or any ocean](#)  
751 [physics.](#) PlankTOM11 offers the first insight into the role of jellyfish [on plankton community structure,](#)  
752 [spatiotemporal dynamics, and biomass,](#) using a global biogeochemical model that represents multiple plankton  
753 functional types.

754

### 755 3.5 CONCLUSION

756

757 Jellyfish have been included as a PFT in a global ocean biogeochemical model for the first time as far as we can  
758 tell at the time of writing. The PlankTOM11 model provides reasonable overall replication of global ecosystem  
759 properties and improved surface chlorophyll, particularly the north/south ratio. The replication of global mean  
760 jellyfish biomass, 0.13 PgC, is within the observational range, and in the region with the highest density of  
761 observations PlankTOM11 closely replicates the mean and seasonal jellyfish biomass. There is a deficit of data  
762 on jellyfish carbon biomass observations and physiological rates. Monitoring and data collection efforts have  
763 increased over recent years; we recommend a further increase especially focussing in less-surveyed regions and  
764 on non-temperate species.



765 The central role of jellyfish is to exert control over the other zooplankton, with the greatest influence on  
766 macrozooplankton. Through trophic cascade mechanisms jellyfish also influence the biomass and spatiotemporal  
767 distribution of phytoplankton. PlankTOM11 is a successful first step in the inclusion of jellyfish in global ocean  
768 biogeochemical modelling. The model raises interesting questions about the sensitivity of the zooplankton  
769 community to changes in jellyfish mortality and calls for a further investigation in interactions between  
770 macrozooplankton and jellyfish. Future model development, alongside POC improvements, could include an  
771 exploration of the life cycle, coastal advantages, and higher resolution ocean physical processes to enhance  
772 patchiness.

773

**Table A1:** Sources and metadata for jellyfish growth rates, including references with associated number of data points, species and life stage used to inform the growth parameter of jellyfish in PlankTOM11.

Reference	<i>n</i>	Species	Life Stage
Båmstedt et al., (1997)	3	<i>Cynea capillata</i>	Ephyrae
Daan (1986)	8	<i>Sarsia tubulosa</i>	Medusae
Frandsen & Riisgård (1997)	5	<i>Aurelia aurita</i>	Medusae
Hansson (1997)	20	<i>Aurelia aurita</i>	Medusae
Møller & Riisgård (2007a)	34	<i>Sarsia tubulosa</i> , <i>Aurelia aurita</i> , <i>Aequorea vitrina</i>	Medusae, ephyrae
Møller & Riisgård (2007b)	10	<i>Aurelia aurita</i>	Medusae, ephyrae
Olesen (1994)	8	<i>Aurelia aurita</i> , <i>Chrysaora</i> <i>quinquecirrha</i>	Medusae, ephyrae
Widmer (2005)	10	<i>Aurelia labiata</i>	Ephyrae

**Table A2:** The fit to the growth data for PFT's for the new three-parameter fit used in this study (see Eq. 3 and Fig. 2) and the two-parameter fit (see Eq. 2 and Fig. 2).

PFT	R <sup>2</sup>		<i>n</i>
	Two-parameter	Three-parameter	
CNI	9.58	11.36	98
MAC	36.57	36.76	253
MES	0.32	0.34	2742
PRO	0.00	7.81	1300
BAC	1.66	1.66	1429
DIA	9.59	9.58	439
PHA	6.29	37.07	67
MIX	21.25	19.17	95
COC	33.91	36.01	322
PIC	20.17	20.29	150
FIX	2.67	10.62	32

**Table A3:** Sources and metadata for jellyfish grazing preferences, including references with associated species, life stage and preference for prey (categorised into PFTs) with any notable phrases used to inform the grazing of jellyfish in PlankTOM11.

Reference	Species/Class/Genera	Life Stage	PFT preference
Båmstedt et al. (2001)	<i>Aurelia aurita</i>	Ephyrae	Mixed-phytoplankton, mesozooplankton and particulate organic material
Colin et al. (2005)	<i>Aglaura hemistoma</i>	Medusa	“microplanktonic omnivores”; protozooplankton and some phytoplankton
Flynn and Gibbons (2007)	<i>Chrysaora hysoscella</i>	Medusa	Wide variety ranging in size from protozooplankton to macrozooplankton, with the “numerically dominant” prey as mesozooplankton
Malej et al. (2007)	<i>Aurelia</i> sp.	Medusa	Mesozooplankton and protozooplankton
Morais et al. (2015)	<i>Blackfordia virginica</i>	Medusa	Mesozooplankton and diatoms
Purcell (1992)	<i>Chrysaora quinquecirrha</i>	Medusa	Mesozooplankton (upto 71% of diet)
Purcell (1997)	Hydromedusa		“mostly generalist feeders”, mesozooplankton as a preference
Purcell (2003)	<i>Aurelia labiata</i> , <i>Cyanea capillata</i> , <i>Aequorea aequorea</i>		Mainly mesozooplankton
Stoecker et al. (1987)	<i>Aurelia aurita</i>	Medusa	Protozooplankton and mesozooplankton preferentially removed from “natural mircozooplankton” assemblage. In cultured prey assemblage, larger protozooplankton were selected.
Uye and Shimauchi (2005b)	<i>Aurelia aurita</i>	Medusa	Mostly mesozooplankton, some protozooplankton
Costello and Colin (2002)	<i>Aglantha digitale</i> , <i>Sarsia tubulosa</i> , <i>Proboscoidactyla flavicirrata</i> , <i>Aequorea victoria</i> , <i>Mitrocoma cellularia</i> , <i>Phialidium gregarium</i>	Medusa	Mesozooplankton (crustacean) and protozooplankton (ciliates)

777

778

779

780

781

782

**Table A4:** Additional tuning parameter values for PlankTOM11 (see Sect.2.1.5) following the change to the growth rate formulation. 'Before growth change' values are those used in PlankTOM10<sup>LQ16</sup> and 'after growth change' values are used in simulations for this study (PlankTOM11, PlankTOM10.5 and PlankTOM10).

Parameter	Before growth change	After growth change
Grazing preference ratio of mesozooplankton for <i>Phaeocystis</i>	0.75	1
Grazing preference ratio of protozooplankton for picophytoplankton	2	3
Half saturation constant of phytoplankton grazing on iron		
Diatoms	40.0e-9	80.0e-9
Picophytoplankton	10.0e-9	25.0e-9
<i>Phaeocystis</i>	25.0e-9	80.0e-9
Half saturation constant of bacteria for dissolved organic carbon	10.0e-6	8.0e-7
Maximum bacteria uptake rate	3.15	1.90
Diatom respiration	0.012	0.12

783  
784  
785  
786  
787  
788  
789  
790  
791  
792  
793  
794  
795

**Table A5.** Global mean values for rates and biomass from observations with the associated references. In parenthesis is the percentage share of the plankton type of the total Phytoplankton or Zooplankton biomass.

	Observations	Reference for the data
<b>Rates</b>		
Primary production (PgC y <sup>-1</sup> )	51-65	Buitenhuis et al. (2013b)
Export production at 100m (PgC y <sup>-1</sup> )	5-13	Henson et al. (2011), Palevsky et al. (2018)
CaCO <sub>3</sub> export at 100m (PgC y <sup>-1</sup> )	0.6-1.1	Lee (2001), Sarmiento et al. (2002)
N <sub>2</sub> fixation (TgN y <sup>-1</sup> )	60-200	Gruber (2008)
<b>Phytoplankton biomass 0-200m (PgC)</b>		
N <sub>2</sub> -fixers	0.008-0.12 (2-8%)	Luo et al. (2012)
Picophytoplankton	0.28-0.52 (35-68%)	Buitenhuis et al. (2012b)
Coccolithophores	0.001-0.032 (0.2-2%)	O'Brien et al. (2013)
Mixed-phytoplankton	-	-
<i>Phaeocystis</i>	0.11-0.69 (27-46%)	Vogt et al. (2012)
Diatoms	0.013-0.75 (3-50%)	Leblanc et al. (2012)
<b>Heterotrophs biomass 0-200m (PgC)</b>		
Bacteria	0.25-0.26	Buitenhuis et al. (2012a)
Protozooplankton	0.10-0.37 (27-31%)	Buitenhuis et al. (2010)
Mesozooplankton	0.21-0.34 (25-66%)	Moriarty and O'Brien (2013)
Macrozooplankton	0.01-0.64 (3-47%)	Moriarty et al. (2013)
Jellyfish zooplankton	0.10-3.11	Bar-On et al. (2018), Lucas et al. (2014), Buitenhuis et al. (2013b)

796

797

798

799

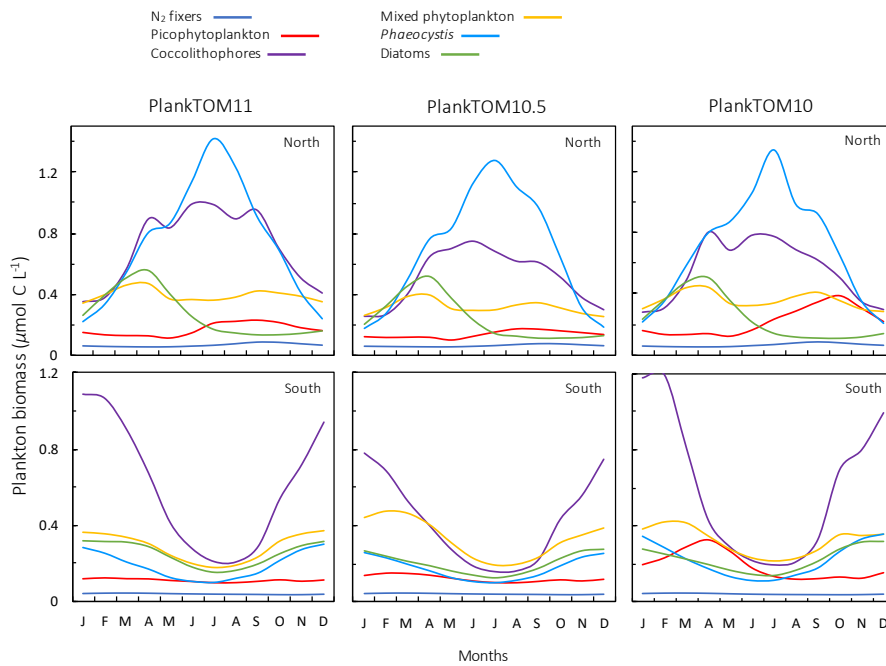
800

**Table A6:** Total phytoplankton biomass ( $\mu\text{mol C L}^{-1}$ ) for  $30^{\circ}\text{N} - 70^{\circ}\text{N}$  across all longitudes. Observations are from gridded MAREDAT, all data are for the surface ocean (0-10 meters). Phytoplankton types include picophytoplankton, *Phaeocystis*, diatoms, nitrogen-fixers and coccolithophores. The seasonal amplitude is the amplitude for the full seasonal cycle (January – December) and the non-winter amplitude is the amplitude for March – October.

	Seasonal Amplitude	Non-winter Amplitude
Observations (median – mean)	0.78 – 2.67	0.70 – 2.12
PlankTOM11	1.82	0.97
PlankTOM10.5	1.54	0.80
PlankTOM10	1.69	0.81
PlankTOM10 <sup>L-Q16</sup>	1.68	1.02

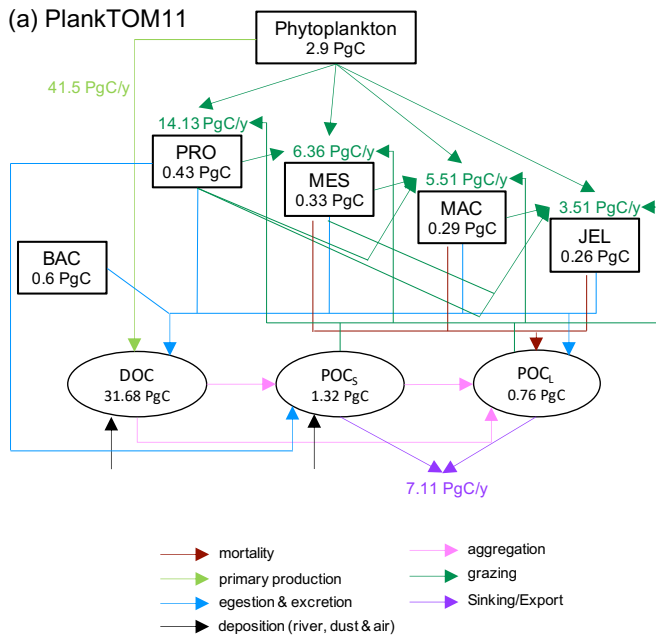
801

802

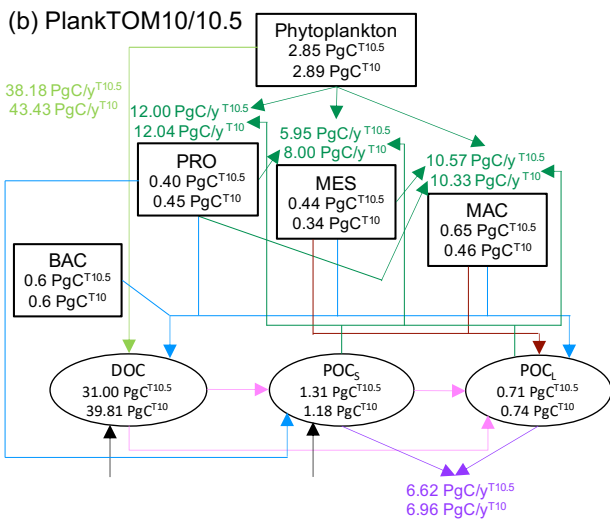


803

804 **Figure A1.** Seasonal surface carbon biomass ( $\mu\text{mol C L}^{-1}$ ) of phytoplankton PFTs;  $\text{N}_2$  fixers, picophytoplankton,  
805 coccolithophores, mixed phytoplankton, *Phaeocystis* and diatoms. Panels shown PFT biomass for PlankTOM11 (left),  
806 PlankTOM10.5 (middle) and PlankTOM10 (right), for two regions; the north  $30^{\circ}\text{N} - 70^{\circ}\text{N}$  (top) and the south  $30^{\circ}\text{S} - 70^{\circ}\text{S}$   
807 across all longitudes. All data are averaged for 1985-2015.



808



809

810 **Figure A2.** Schematic representation of global carbon biomass and rates in the PlankTOM marine ecosystem model including  
 811 sources and sinks for dissolved organic carbon (DOC) and small (POC<sub>s</sub>) and large (POC<sub>l</sub>) particulate organic carbon. (a)  
 812 PlankTOM11 and (b) PlankTOM10 and PlankTOM10.5. Carbon biomass (PgC) of PFT's and organic carbon pools are given  
 813 within boxes and ovals, carbon rates (PgC/y) of primary production (light green), grazing (dark green) and export production  
 814 (purple) are given next to the corresponding arrows. All data are averaged for 1985 to 2015.

815 **Author Contribution**

816 RMW, CLQ, ETB and SP conceptualized the research goals and aims. RMW carried out the formal analysis  
817 with contributions from CLQ and ETB. RW developed the model code with significant contributions from ETB,  
818 and RMW performed the simulations. RMW prepared the manuscript with contributions from all co-authors.

819 The authors declare that they have no conflict of interest.

820

821 **Acknowledgements**

822 RMW was funded by Doctoral Training Programme ARIES, funded by the UK Natural Environment Research  
823 Council (project no. NE/L002582/1). CLQ was funded by the Royal Society (grant no. RP/R1191063). ETB  
824 was funded by the European Commission H2020 project CRESCENDO (grant no. 641816). This research was  
825 partly conducted in South Africa with the support of the Newton International PhD exchange programme (grant  
826 no. ES/N013948/1). The model simulations were done on the UEA's High Performance Computing Cluster.

827



828 **References**

- 829 Acevedo, M. J., Fuentes, V. L., Olariaga, A., Canepa, A., Belmar, M. B., Bordehore, C. and Calbet, A.:  
830 Maintenance, feeding and growth of *Carybdea marsupialis* (Cnidaria: Cubozoa) in the laboratory, *J. Exp. Mar.*  
831 *Bio. Ecol.*, 439, 84–91, doi:<https://doi.org/10.1016/j.jembe.2012.10.007>, 2013.
- 832 Acuña, J. L., López-Urrutia, Á. and Colin, S.: Faking giants: The evolution of high prey clearance rates in  
833 jellyfishes, *Science* (80-. ), 333(6049), 1627–1629, doi:[10.1126/science.1205134](https://doi.org/10.1126/science.1205134), 2011.
- 834 Almeda, R., Wambaugh, Z., Chai, C., Wang, Z., Liu, Z. and Buskey, E. J.: Effects of crude oil exposure on  
835 bioaccumulation of polycyclic aromatic hydrocarbons and survival of adult and larval stages of gelatinous  
836 zooplankton, *PLoS One*, 8(10), e74476, 2013.
- 837 Antonov, J. I., Seidov, D., Boyer, T., Locarnini, R., Mishonov, A., Garcia, H., Baranova, O., Zweng, M. and  
838 Johnson, D.: *World Ocean Atlas 2009*, S. Levitus, Ed. NOAA Atlas NESDIS 69, U.S. Government Printing  
839 Office, Washington, D.C., 2010.
- 840 Bamstedt, U., Ishii, H. and Martinussen, M. B.: Is the Scyphomedusa *Cyanea capillata* (L.) dependent on  
841 gelatinous prey for its early development?, *Sarsia*, (May 1996), 1997.
- 842 Bámstedt, U., Wild, B. and Martinussen, M. B.: Significance of food type for growth of ephyrae *Aurelia aurita*  
843 (Scyphozoa), *Mar. Biol.*, 139(4), 641–650, doi:[10.1007/s002270100623](https://doi.org/10.1007/s002270100623), 2001.
- 844 Bar-On, Y. M., Phillips, R. and Milo, R.: The biomass distribution on Earth, *Proc. Natl. Acad. Sci. U. S. A.*,  
845 115(25), 6506–6511, doi:[10.1073/pnas.1711842115](https://doi.org/10.1073/pnas.1711842115), 2018.
- 846 Benedetti-Cecchi, L., Canepa, A., Fuentes, V., Tamburello, L., Purcell, J. E., Piraino, S., Roberts, J., Boero, F.  
847 and Halpin, P.: Deterministic Factors Overwhelm Stochastic Environmental Fluctuations as Drivers of Jellyfish  
848 Outbreaks, *PLoS One*, 10(10), e0141060, 2015.
- 849 Billett, D. S. M., Bett, B. J., Jacobs, C. L., Rouse, I. P. and Wigham, B. D.: Mass deposition of jellyfish in the  
850 deep Arabian Sea, *Limnol. Oceanogr.*, 51(5), 2077–2083, 2006.
- 851 Boero, F., Bucci, C., Colucci, A. M. R., Gravili, C. and Stabili, L.: *Obelia* (Cnidaria, Hydrozoa,  
852 *Campanulariidae*): A microphagous, filter-feeding medusa, *Mar. Ecol.*, 28(SUPPL. 1), 178–183,  
853 doi:[10.1111/j.1439-0485.2007.00164.x](https://doi.org/10.1111/j.1439-0485.2007.00164.x), 2007.
- 854 Boero, F., Bouillon, J., Gravili, C., Miglietta, M. P., Parsons, T. and Piraino, S.: Gelatinous plankton:  
855 irregularities rule the world (sometimes), *Mar. Ecol. Prog. Ser.*, 356, 299–310, doi:[10.3354/meps07368](https://doi.org/10.3354/meps07368), 2008.
- 856 Boero, F., Brotz, L., Gibbons, M. J., Piraino, S. and Zampardi, S.: Impacts and effects of ocean warming on  
857 jellyfish, in *Explaining Ocean Warming: Causes, scale, effects and consequences*, pp. 213–237, IUCN, Gland,  
858 Switzerland., 2016.
- 859 Brotz, L., Cheung, W. W. L., Kleisner, K., Pakhomov, E. and Pauly, D.: Increasing jellyfish populations: trends  
860 in Large Marine Ecosystems, *Hydrobiologia*, 690(1), 3–20, doi:[10.1007/s10750-012-1039-7](https://doi.org/10.1007/s10750-012-1039-7), 2012.

861 Buitenhuis, E. T., Le Quéré, C., Aumont, O., Beaugrand, G., Bunker, A., Hirst, A., Ikeda, T., O'Brien, T.,  
862 Piontkovski, S. and Straile, D.: Biogeochemical fluxes through mesozooplankton, *Global Biogeochem. Cycles*,  
863 20(2), 2006.

864 Buitenhuis, E. T., Rivkin, R. B., Sailley, S. and Le Quéré, C.: Biogeochemical fluxes through  
865 microzooplankton, *Global Biogeochem. Cycles*, 24(4), doi:10.1029/2009GB003601, 2010.

866 Buitenhuis, E. T., Li, W. K. W., Lomas, M. W., Karl, D. M., Landry, M. R. and Jacquet, S.: Picoheterotroph  
867 (Bacteria and Archaea) biomass distribution in the global ocean, *Earth Syst. Sci. Data*, 4(1), 101–106,  
868 doi:10.5194/essd-4-101-2012, 2012a.

869 Buitenhuis, E. T., Li, W. K. W., Vaulot, D., Lomas, M. W., Landry, M. R., Partensky, F., Karl, D. M., Ulloa, O.,  
870 Campbell, L., Jacquet, S., Lantoine, F., Chavez, F., MacIas, D., Gosselin, M. and McManus, G. B.:  
871 Picophytoplankton biomass distribution in the global ocean, *Earth Syst. Sci. Data*, 4(1), 37–46,  
872 doi:10.5194/essd-4-37-2012, 2012b.

873 Buitenhuis, E. T., Hashioka, T. and Le Quéré, C.: Combined constraints on global ocean primary production  
874 using observations and models, *Global Biogeochem. Cycles*, 27(3), 847–858, doi:10.1002/gbc.20074, 2013a.

875 Buitenhuis, E. T., Vogt, M., Moriarty, R., Bednarsek, N., Doney, S. C., Leblanc, K., Le Quéré, C., Luo, Y. W.,  
876 O'Brien, C., O'Brien, T., Peloquin, J., Schiebel, R. and Swan, C.: MAREDAT: towards a world atlas of  
877 MARine Ecosystem DATA, *Earth Syst. Sci. Data*, 5(2), 227–239, doi:10.5194/essd-5-227-2013, 2013b.

878 Chelsky, A., Pitt, K. A. and Welsh, D. T.: Biogeochemical implications of decomposing jellyfish blooms in a  
879 changing climate, *Estuar. Coast. Shelf Sci.*, 154, 77–83, doi:10.1016/j.ecss.2014.12.022, 2015.

880 Chiaverano, L. M., Robinson, K. L., Tam, J., Ruzicka, J. J., Quiñones, J., Aleksa, K. T., Hernandez, F. J.,  
881 Brodeur, R. D., Leaf, R. and Uye, S.: Evaluating the role of large jellyfish and forage fishes as energy pathways,  
882 and their interplay with fisheries, in the Northern Humboldt Current System, *Prog. Oceanogr.*, 164, 28–36,  
883 2018.

884 Colin, S. P., Costello, J. H., Graham, W. M. and Higgins III, J.: Omnivory by the small cosmopolitan  
885 hydromedusa *Aglaura hemistoma*, *Limnol. Oceanogr.*, 50(4), 1264–1268, 2005.

886 Condon, R. H., Steinberg, D. K., Del Giorgio, P. A., Bouvier, T. C., Bronk, D. A., Graham, W. M. and  
887 Ducklow, H. W.: Jellyfish blooms result in a major microbial respiratory sink of carbon in marine systems,  
888 *Proc. Natl. Acad. Sci. U. S. A.*, 108(25), 10225–10230, doi:10.1073/pnas.1015782108, 2011.

889 Condon, R. H., Graham, W. M., Duarte, C. M., Pitt, K. A., Lucas, C. H., Haddock, S. H. D., Sutherland, K. R.,  
890 Robinson, K. L., Dawson, M. N., Beth, M., Decker, M. B., Mills, C. E., Purcell, J. E., Malej, A., Mianzan, H.,  
891 Uye, S.-I., Gelcich, S. and Madin, L. P.: Questioning the Rise of Gelatinous Zooplankton in the World's  
892 Oceans, *Bioscience*, 62(2), 160–169, doi:10.1525/bio.2012.62.2.9, 2012.

893 Condon, R. H., Duarte, C. M., Pitt, K. A., Robinson, K. L., Lucas, C. H., Sutherland, K. R., Mianzan, H. W.,  
894 Bogeberg, M., Purcell, J. E., Decker, M. B., Uye, S., Madin, L. P., Brodeur, R. D., Haddock, S. H. D., Malej,

895 A., Parry, G. D., Eriksen, E., Quiñones, J., Acha, M., Harvey, M., Arthur, J. M. and Graham, W. M.: Recurrent  
896 jellyfish blooms are a consequence of global oscillations., *Proc. Natl. Acad. Sci. U. S. A.*, 110(3), 1000–5,  
897 doi:10.1073/pnas.1210920110, 2013.

898 Costello, J. H. and Colin, S. P.: Prey resource use by coexistent hydromedusae from Friday Harbor,  
899 Washington, *Limnol. Oceanogr.*, 47(4), 934–942, doi:10.4319/lo.2002.47.4.0934, 2002.

900 Crum, K. P., Fuchs, H. L., Bologna, P. A. X. and Gaynor, J. J.: Model-to-data comparisons reveal influence of  
901 jellyfish interactions on plankton community dynamics, *Mar. Ecol. Prog. Ser.*, 517, 105–119,  
902 doi:10.3354/meps11022, 2014.

903 Daan, R.: Food intake and growth of *sarsia tubulosa* (sars, 1835), with quantitative estimates of predation on  
904 copepod populations, *Netherlands J. Sea Res.*, 20(1), 67–74, 1986.

905 Doney, S. C., Ruckelshaus, M., Duffy, J. E., Barry, J. P., Chan, F., English, C. A., Galindo, H. M., Grebmeier, J.  
906 M., Hollowed, A. B., Knowlton, N., Polovina, J., Rabalais, N. N., Sydeman, W. J. and Talley, L. D.: Climate  
907 Change Impacts on Marine Ecosystems, *Annu. Rev. Mar. Sci.* Vol 4, 4, 11–37, doi:10.1146/annurev-marine-  
908 041911-111611, 2012.

909 Duarte, C. M., Pitt, K. A. and Lucas, C. H.: Understanding Jellyfish Blooms, in *Jellyfish Blooms*, edited by C.  
910 M. Pitt, Kylie A, Lucas, pp. 1–5, Springer, London. [online] Available from:  
911 <http://www.springer.com/life+sciences/ecology/book/978-94-007-7014-0>, 2013.

912 Flynn, B. A. and Gibbons, M. J.: A note on the diet and feeding of *Chrysaora hysoscella* in Walvis Bay Lagoon,  
913 Namibia, during September 2003, *African J. Mar. Sci.*, 29(2), 303–307, doi:10.2989/AJMS.2007.29.2.15.197,  
914 2007.

915 Fossette, S., Gleiss, A. C., Chalumeau, J., Bastian, T., Armstrong, C. D., Vandenabeele, S., Karpytchev, M. and  
916 Hays, G. C.: Current-Oriented Swimming by Jellyfish and Its Role in Bloom Maintenance, *Curr. Biol.*, 25(3),  
917 342–347, doi:10.1016/j.cub.2014.11.050, 2015.

918 Frandsen, K. T. and Riisgård, H. U.: Size dependent respiration and growth of jellyfish, *Aurelia aurita*, *Sarsia*,  
919 82(4), 307–312, doi:10.1080/00364827.1997.10413659, 1997.

920 Gibbons, M. J. and Richardson, A. J.: Beyond the jellyfish joyride and global oscillations: advancing jellyfish  
921 research, *J. Plankton Res.*, 35(5), 929–938, doi:10.1093/plankt/ftb063, 2013.

922 Graham, W. M., Pagès, F. and Hamner, W.: A physical context for gelatinous zooplankton aggregations: a  
923 review, *Hydrobiologia*, 451(1–3), 199–212, doi:10.1023/A:1011876004427, 2001.

924 Gruber, N.: The Marine Nitrogen Cycle: Overview and Challenges, *Nitrogen Mar. Environ.*, 1–50,  
925 doi:10.1016/B978-0-12-372522-6.00001-3, 2008.

926 Hamner, W. M. and Dawson, M. N.: A review and synthesis on the systematics and evolution of jellyfish  
927 blooms: advantageous aggregations and adaptive assemblages, *Hydrobiologia*, 616, 161–191,

928 doi:10.1007/s10750-008-9620-9, 2009.

929 Han, C.-H. and Uye, S.: Combined effects of food supply and temperature on asexual reproduction and somatic  
930 growth of polyps of the common jellyfish *Aurelia aurita* sl, *Plankt. Benthos Res.*, 5(3), 98–105, 2010.

931 Hansson, L. J.: Effect of temperature on growth rate of *Aurelia aurita* (Cnidaria, Scyphozoa) from  
932 Gullmarsfjorden, Sweden, *Mar. Ecol. Prog. Ser.*, 161, 145–153, doi:10.3354/meps161145, 1997.

933 Hansson, L. J. and Norrman, B.: Release of dissolved organic carbon (DOC) by the scyphozoan jellyfish  
934 *Aurelia aurita* and its potential influence on the production of planktic bacteria, *Mar. Biol.*, 121(3), 527–532,  
935 doi:10.1007/BF00349462, 1995.

936 [Heneghan, R. F., Everett, J. D., Sykes, P., Batten, S. D., Edwards, M., Takahashi, K., Suthers, I. M., Blanchard,](#)  
937 [J. L. and Richardson, A. J.: A functional size-spectrum model of the global marine ecosystem that resolves](#)  
938 [zooplankton composition. \*Ecol. Modell.\*, 435\(August\), 109265, doi:10.1016/j.ecolmodel.2020.109265. 2020.](#)

939 Henschke, N., Stock, C. A. and Sarmiento, J. L.: Modeling population dynamics of scyphozoan jellyfish  
940 (*Aurelia* spp.) in the Gulf of Mexico, *Mar. Ecol. Prog. Ser.*, 591, 167–183, doi:10.3354/meps12255, 2018.

941 Henson, S. A., Sanders, R., Madsen, E., Morris, P. J., Le Moigne, F. and Quartly, G. D.: A reduced estimate of  
942 the strength of the ocean's biological carbon pump, *Geophys. Res. Lett.*, 38(4), 10–14,  
943 doi:10.1029/2011GL046735, 2011.

944 Hirst, A. G. and Kiørboe, T.: Mortality of marine planktonic copepods: global rates and patterns, *Mar. Ecol.*  
945 *Prog. Ser.*, 230, 195–209, 2002.

946 Ikeda, T.: Metabolic rates of epipelagic marine zooplankton as a function of body mass and temperature, *Mar.*  
947 *Biol.*, 85(1), 1–11, 1985.

948 Kalnay, E., Kanamitsu, M., Kistler, R., Collins, W., Deaven, D., Gandin, L., Iredell, M., Saha, S., White, G. and  
949 Woollen, J.: The NCEP/NCAR 40-year reanalysis project, *Bull. Am. Meteorol. Soc.*, 77(3), 437–472, 1996.

950 Key, R. M., Kozyr, A., Sabine, C. L., Lee, K., Wanninkhof, R., Bullister, J. L., Feely, R. A., Millero, F. J.,  
951 Mordy, C. and Peng, T.: A global ocean carbon climatology: Results from Global Data Analysis Project  
952 (GLODAP), *Global Biogeochem. Cycles*, 18(4), 2004.

953 Kriest, I. and Oschlies, A.: On the treatment of particulate organic matter sinking in large-scale models of  
954 marine biogeochemical cycles, *Biogeosciences (BG)*, 5, 55–72, 2008.

955 Lamb, P. D., Hunter, E., Pinnegar, J. K., Creer, S., Davies, R. G. and Taylor, M. I.: Jellyfish on the menu:  
956 mtDNA assay reveals scyphozoan predation in the Irish Sea, *R. Soc. Open Sci.*, 4(11), doi:10.1098/rsos.171421,  
957 2017.

958 Leblanc, K., Arístegui, J., Armand, L., Assmy, P., Beker, B., Bode, A., Breton, E., Cornet, V., Gibson, J.,  
959 Gosselin, M. P., Kopczynska, E., Marshall, H., Peloquin, J., Piontkovski, S., Poulton, A. J., Quéguiner, B.,  
960 Schiebel, R., Shipe, R., Stefels, J., Van Leeuwe, M. A., Varela, M., Widdicombe, C. and Yallop, M.: A global

961 diatom database- A bundance, biovolume and biomass in the world ocean, *Earth Syst. Sci. Data*, 4(1), 149–165,  
962 doi:10.5194/essd-4-149-2012, 2012.

963 Lebrato, M., Pitt, K. A., Sweetman, A. K., Jones, D. O. B., Cartes, J. E., Oschlies, A., Condon, R. H., Molinero,  
964 J. C., Adler, L., Gaillard, C., Lloris, D. and Billett, D. S. M.: Jelly-falls historic and recent observations: a  
965 review to drive future research directions, *Hydrobiologia*, 690(1), 227–245, doi:10.1007/s10750-012-1046-8,  
966 2012.

967 Lebrato, M., Mendes, P. de J., Steinberg, D. K., Cartes, J. E., Jones, B. M., Birsa, L. M., Benavides, R. and  
968 Oschlies, A.: Jelly biomass sinking speed reveals a fast carbon export mechanism, *Limnol. Oceanogr.*, 58(3),  
969 1113–1122, 2013a.

970 Lebrato, M., Molinero, J.-C., Cartes, J. E., Lloris, D., Mélin, F. and Beni-Casadella, L.: Sinking jelly-carbon  
971 unveils potential environmental variability along a continental margin, *PLoS One*, 8(12), e82070, 2013b.

972 Lee, K.: Global net community production estimated from the annual cycle of surface water total dissolved  
973 inorganic carbon, *Limnol. Oceanogr.*, 46(6), 1287–1297, doi:10.4319/lo.2001.46.6.1287, 2001.

974 Lilley, M. K. S., Beggs, S. E., Doyle, T. K., Hobson, V. J., Stromberg, K. H. P. and Hays, G. C.: Global patterns  
975 of epipelagic gelatinous zooplankton biomass, *Mar. Biol.*, 158(11), 2429–2436, doi:10.1007/s00227-011-1744-  
976 1, 2011.

977 Lucas, C. H. and Dawson, M. N.: What Are Jellyfishes and Thaliaceans and Why Do They Bloom?, in *Jellyfish*  
978 *blooms*, pp. 9–44, Springer., 2014.

979 Lucas, C. H., Graham, W. M. and Widmer, C.: Jellyfish Life Histories: role of polyps in forming and  
980 maintaining scyphomedusa populations, *Adv. Mar. Biol. Vol 63*, 63, 133–196, doi:10.1016/b978-0-12-394282-  
981 1.00003-x, 2012.

982 Lucas, C. H., Jones, D. O. B., Hollyhead, C. J., Condon, R. H., Duarte, C. M., Graham, W. M., Robinson, K. L.,  
983 Pitt, K. A., Schildhauer, M. and Regetz, J.: Gelatinous zooplankton biomass in the global oceans: geographic  
984 variation and environmental drivers, *Glob. Ecol. Biogeogr.*, 23(7), 701–714, doi:10.1111/geb.12169, 2014.

985 Luo, J. Y., Condon, R. H., Stock, C. A., Duarte, C. M., Lucas, C. H., Pitt, K. A. and Cowen, R. K.: Gelatinous  
986 Zooplankton-Mediated Carbon Flows in the Global Oceans: A Data-Driven Modeling Study, *Global*  
987 *Biogeochem. Cycles*, 34(9), doi:10.1029/2020GB006704, 2020.

988 Luo, Y. W., Doney, S. C., Anderson, L. A., Benavides, M., Berman-Frank, I., Bode, A., Bonnet, S., Boström, K.  
989 H., Böttjer, D., Capone, D. G., Carpenter, E. J., Chen, Y. L., Church, M. J., Dore, J. E., Falcón, L. I., Fernández,  
990 A., Foster, R. A., Furuya, K., Gómez, F., Gunderson, K., Hynes, A. M., Karl, D. M., Kitajima, S., Langlois, R.  
991 J., Laroche, J., Letelier, R. M., Marañón, E., McGillicuddy, D. J., Moisander, P. H., Moore, C. M., Mourinõ-  
992 Carballido, B., Mulholland, M. R., Needoba, J. A., Orcutt, K. M., Poulton, A. J., Rahav, E., Raimbault, P., Rees,  
993 A. P., Riemann, L., Shiozaki, T., Subramaniam, A., Tyrrell, T., Turk-Kubo, K. A., Varela, M., Villareal, T. A.,  
994 Webb, E. A., White, A. E., Wu, J. and Zehr, J. P.: Database of diazotrophs in global ocean: Abundance, biomass  
995 and nitrogen fixation rates, *Earth Syst. Sci. Data*, 4(1), 47–73, doi:10.5194/essd-4-47-2012, 2012.

- 996 Madec, G.: NEMO ocean engine, Note du Pole modélisation Inst. Pierre-Simon Laplace, 27 [online] Available  
997 from: <https://doi.org/10.5281/zenodo.1464817>, 2013.
- 998 Malej, A. and Malej, M.: Population dynamics of the jellyfish *Pelagia noctiluca* (Forsskål, 1775), in *Marine*  
999 *Eutrophication and Populations Dynamics*, edited by G. Colombo Ferrara, I., pp. 215–219, Denmark., 1992.
- 1000 Malej, A., Turk, V., Lučić, D. and Benović, A.: Direct and indirect trophic interactions of *Aurelia*  
1001 sp.(Scyphozoa) in a stratified marine environment (Mljet Lakes, Adriatic Sea), *Mar. Biol.*, 151(3), 827–841,  
1002 2007.
- 1003 Martell, L., Piraino, S., Gravili, C. and Boero, F.: Life cycle, morphology and medusa ontogenesis of *Turritopsis*  
1004 *dohrnii* (Cnidaria: Hydrozoa), *Ital. J. Zool.*, 83(3), 390–399, doi:10.1080/11250003.2016.1203034, 2016.
- 1005 Mills, C. E.: Natural mortality in NR Pacific coastal hydromedusae - grazing predation, wound-healing and  
1006 senescence, *Bull. Mar. Sci.*, 53(1), 194–203, 1993.
- 1007 Møller, L. F. and Riisgård, H. U.: Feeding, bioenergetics and growth in the common jellyfish *Aurelia aurita* and  
1008 two hydromedusae, *Sarsia tubulosa* and *Aequorea vitrina*, *Mar. Ecol. Prog. Ser.*, 346, 167–177,  
1009 doi:10.3354/meps06959, 2007a.
- 1010 Møller, L. F. and Riisgård, H. U.: Population dynamics, growth and predation impact of the common jellyfish  
1011 *Aurelia aurita* and two hydromedusae, *Sarsia tubulosa*, and *Aequorea vitrina* in Limfjorden (Denmark), *Mar.*  
1012 *Ecol. Prog. Ser.*, 346, 153–165, doi:10.3354/meps06960, 2007b.
- 1013 Morais, P., Parra, M. P., Marques, R., Cruz, J., Angélico, M. M., Chainho, P., Costa, J. L., Barbosa, A. B. and  
1014 Teodósio, M. A.: What are jellyfish really eating to support high ecophysiological condition?, *J. Plankton Res.*,  
1015 37(5), 1036–1041, doi:10.1093/plankt/fbv044, 2015.
- 1016 Moriarty, R.: The role of macro-zooplankton in the global carbon cycle, Ph.D. Thesis, School of Environmental  
1017 Sciences, University of East Anglia, England., 2009.
- 1018 Moriarty, R. and O'Brien, T. D.: Distribution of mesozooplankton biomass in the global ocean, *Earth Syst. Sci.*  
1019 *Data*, 5(1), 45–55, doi:10.5194/essd-5-45-2013, 2013.
- 1020 Moriarty, R., Buitenhuis, E. T., Le Quéré, C. and Gosselin, M. P.: Distribution of known macrozooplankton  
1021 abundance and biomass in the global ocean, *Earth Syst. Sci. Data*, 5(2), 241–257, doi:10.5194/essd-5-241-2013,  
1022 2013.
- 1023 O'Brien, C. J., Peloquin, J. A., Vogt, M., Heinle, M., Gruber, N., Ajani, P., Andruleit, H., Aristegui, J.,  
1024 Beaufort, L., Estrada, M., Karentz, D., Kopczyńska, E., Lee, R., Poulton, A. J., Pritchard, T. and Widdicombe,  
1025 C.: Global marine plankton functional type biomass distributions: Coccolithophores, *Earth Syst. Sci. Data*, 5(2),  
1026 259–276, doi:10.5194/essd-5-259-2013, 2013.
- 1027 Olesen, N. J., Frandsen, K. and Riisgard, H. U.: Population dynamics, growth and energetics of jellyfish *Aurelia*  
1028 *aurita* in a shallow fjord, *Mar. Ecol. Prog. Ser.*, 105(1–2), 9–18, doi:10.3354/meps105009, 1994.

- 1029 Palevsky, H. I. and Doney, S. C.: How choice of depth horizon influences the estimated spatial patterns and  
1030 global magnitude of ocean carbon export flux, *Geophys. Res. Lett.*, 45(9), 4171–4179, 2018.
- 1031 Pauly, D., Graham, W., Libralato, S., Morissette, L. and Palomares, M. L. D.: Jellyfish in ecosystems, online  
1032 databases, and ecosystem models, *Hydrobiologia*, 616, 67–85, doi:10.1007/s10750-008-9583-x, 2009.
- 1033 Pitt, K. A., Kingsford, M. J., Rissik, D. and Koop, K.: Jellyfish modify the response of planktonic assemblages  
1034 to nutrient pulses, *Mar. Ecol. Prog. Ser.*, 351, 1–13, doi:10.3354/meps07298, 2007.
- 1035 Pitt, K. A., Welsh, D. T. and Condon, R. H.: Influence of jellyfish blooms on carbon, nitrogen and phosphorus  
1036 cycling and plankton production, *Hydrobiologia*, 616(1), 133–149, 2009.
- 1037 Pitt, K. A., Budarf, A. C., Browne, J. G., Condon, R. H., Browne, D. G. and Condon, R. H.: Bloom and Bust:  
1038 Why Do Blooms of Jellyfish Collapse?, in *Jellyfish Blooms*, edited by C. M. Pitt, Kylie A, Lucas, pp. 79–103,  
1039 Springer, London. [online] Available from: <http://www.springer.com/life+sciences/ecology/book/978-94-007-7014-0>, 2014.
- 1041 Pitt, K. A., Lucas, C. H., Condon, R. H., Duarte, C. M. and Stewart-Koster, B.: Claims that anthropogenic  
1042 stressors facilitate jellyfish blooms have been amplified beyond the available evidence: a systematic review,  
1043 *Front. Mar. Sci.*, 5, 451, 2018.
- 1044 Purcell, J. E.: Effects of predation by the Scyphomedusan *Chrysaora-quinquahirra* on zooplankton populations  
1045 in Chesapeake Bay, USA, *Mar. Ecol. Prog. Ser.*, 87(1–2), 65–76, doi:10.3354/meps087065, 1992.
- 1046 Purcell, J. E.: Pelagic cnidarians and ctenophores as predators: Selective predation, feeding rates, and effects on  
1047 prey populations, *Ann. L Inst. Oceanogr.*, 73(2), 125–137, 1997.
- 1048 Purcell, J. E.: Predation on zooplankton by large jellyfish, *Aurelia labiata*, *Cyanea capillata* and *Aequorea*  
1049 *aequorea*, in Prince William Sound, Alaska, *Mar. Ecol. Prog. Ser.*, 246, 137–152, doi:10.3354/meps246137,  
1050 2003.
- 1051 Purcell, J. E.: Extension of methods for jellyfish and ctenophore trophic ecology to large-scale research, in  
1052 *Jellyfish Blooms: Causes, Consequences, and Recent Advances SE - 3*, vol. 206, edited by K. Pitt and J. Purcell,  
1053 pp. 23–50, Springer Netherlands., 2009.
- 1054 Purcell, J. E., Uye, S. and Lo, W.-T.: Anthropogenic causes of jellyfish blooms and their direct consequences  
1055 for humans: a review, *Mar. Ecol. Prog. Ser.*, 350, 153–174, doi:10.3354/meps07093, 2007.
- 1056 Purcell, J. E., Fuentes, V., Atienza, D., Tilves, U., Astorga, D., Kawahara, M. and Hays, G. C.: Use of  
1057 respiration rates of scyphozoan jellyfish to estimate their effects on the food web, *Hydrobiologia*, 645(1), 135–  
1058 152, 2010.
- 1059 Le Quéré, C., Harrison, S. P., Colin Prentice, I., Buitenhuis, E. T., Aumont, O., Bopp, L., Claustre, H., Cotrim  
1060 Da Cunha, L., Geider, R., Giraud, X., Klaas, C., Kohfeld, K. E., Legendre, L., Manizza, M., Platt, T., Rivkin, R.  
1061 B., Sathyendranath, S., Uitz, J., Watson, A. J. and Wolf-Gladrow, D.: Ecosystem dynamics based on plankton

1062 functional types for global ocean biogeochemistry models, *Glob. Chang. Biol.*, 11(11), 2016–2040,  
1063 doi:10.1111/j.1365-2486.2005.1004.x, 2005.

1064 Le Quéré, C., Takahashi, T., Buitenhuis, E. T., Rödenbeck, C. and Sutherland, S. C.: Impact of climate change  
1065 and variability on the global oceanic sink of CO<sub>2</sub>, *Global Biogeochem. Cycles*, 24(4), 1–10,  
1066 doi:10.1029/2009GB003599, 2010.

1067 Le Quéré, C., Buitenhuis, E. T., Moriarty, R., Alvain, S., Aumont, O., Bopp, L., Chollet, S., Enright, C.,  
1068 Franklin, D. J., Geider, R. J., Harrison, S. P., Hirst, A., Larsen, S., Legendre, L., Platt, T., Prentice, I. C., Rivkin,  
1069 R. B., Sathyendranath, S., Stephens, N., Vogt, M., Salliey, S. and Vallina, S. M.: Role of zooplankton dynamics  
1070 for Southern Ocean phytoplankton biomass and global biogeochemical cycles, *Biogeosciences*, 13, 4111–4133,  
1071 doi:10.5194/bgd-12-11935-2015, 2016.

1072 Ramirez-Romero, E., Molinero, J. C., Paulsen, M., Javidpour, J., Clemmesen, C. and Sommer, U.: Quantifying  
1073 top-down control and ecological traits of the scyphozoan *Aurelia aurita* through a dynamic plankton model, *J.*  
1074 *Plankton Res.*, 40(6), 678–692, 2018.

1075 Rhein, M., Rintoul, S. R., Aoki, S., Campos, E., Chambers, D., Feely, R. A., Gulev, S., Johnson, G. C., Josey, S.  
1076 A., Kostianoy, A., Mauritzen, C., Roemmich, D., Talley, L. D. and Wang, F.: *Observations: Ocean*, edited by T.  
1077 F. Stocker, D. Qin, G.-K. Plattner, M. Tignor, S.K. Allen, J. Boschung, A. Nauels, Y. Xia, V. Bex and P.M.  
1078 Midgley, Cambridge University Press, Cambridge, United Kingdom and New York, NY, USA., 2013.

1079 Richardson, A. J. and Gibbons, M. J.: Are jellyfish increasing in response to ocean acidification?, *Limnol.*  
1080 *Oceanogr.*, 53(5), 2040–2045, 2008.

1081 Rosa, S., Pansera, M., Granata, A. and Guglielmo, L.: Interannual variability, growth, reproduction and feeding  
1082 of *Pelagia noctiluca* (Cnidaria: Scyphozoa) in the Straits of Messina (Central Mediterranean Sea): Linkages with  
1083 temperature and diet, *J. Mar. Syst.*, 111, 97–107, doi:http://dx.doi.org/10.1016/j.jmarsys.2012.10.001, 2013.

1084 Roux, J.-P., van der Lingen, C. D., Gibbons, M. J., Moroff, N. E., Shannon, L. J., Smith, A. D. M. and Cury, P.  
1085 M.: Jellyfication of marine ecosystems as a likely consequence of overfishing small pelagic fishes: lessons from  
1086 the Benguela, *Bull. Mar. Sci.*, 89(1), 249–284, 2013.

1087 Roux, J. P. and Shannon, L. J.: Ecosystem approach to fisheries management in the northern Benguela: the  
1088 Namibian experience, *African J. Mar. Sci.*, 26(1), 79–93, 2004.

1089 Ruzicka, J. J., Brodeur, R. D., Emmett, R. L., Steele, J. H., Zamon, J. E., Morgan, C. A., Thomas, A. C. and  
1090 Wainwright, T. C.: Interannual variability in the Northern California Current food web structure: Changes in  
1091 energy flow pathways and the role of forage fish, euphausiids, and jellyfish, *Prog. Oceanogr.*, 102, 19–41,  
1092 doi:10.1016/j.pocean.2012.02.002, 2012.

1093 Sarmiento, J. L., Dunne, J., Gnanadesikan, A., Key, R. M., Matsumoto, K. and Slater, R.: A new estimate of the  
1094 CaCO<sub>3</sub> to organic carbon export ratio, *Global Biogeochem. Cycles*, 16(4), 54-1-54–12,  
1095 doi:10.1029/2002gb001919, 2002.



1096 Schnedler-Meyer, N. A., Kiørboe, T. and Mariani, P.: Boom and Bust: Life History, Environmental Noise, and  
1097 the (un)Predictability of Jellyfish Blooms, *Front. Mar. Sci.*, 5(257), doi:10.3389/fmars.2018.00257, 2018.

1098 Schoemann, V., Becquevort, S., Stefels, J., Rousseau, V. and Lancelot, C.: Phaeocystis blooms in the global  
1099 ocean and their controlling mechanisms: a review, *J. Sea Res.*, 53(1), 43–66,  
1100 doi:https://doi.org/10.1016/j.seares.2004.01.008, 2005.

1101 Shannon, L. J., Coll, M., Neira, S., Cury, P. and Roux, J.-P.: Chapter 8: Impacts of fishing and climate change  
1102 explored using trophic models, in *Climate Change and Small Pelagic Fish*, edited by C. R. D.M. Checkley J.  
1103 Alheit and Y. Oozeki, pp. 158–190, Cambridge University Press, Cambridge., 2009.

1104 Stoecker, D. K., Michaels, A. E. and Davis, L. H.: Grazing by the jellyfish, *Aurelia aurita*, on microzooplankton,  
1105 *J. Plankton Res.*, 9(5), 901–915, doi:10.1093/plankt/9.5.901, 1987.

1106 Timmermann, R., Goosse, H., Madec, G., Fichefet, T., Ethe, C. and Duliere, V.: On the representation of high  
1107 latitude processes in the ORCA-LIM global coupled sea ice–ocean model, *Ocean Model.*, 8(1–2), 175–201,  
1108 2005.

1109 Uye, S. and Shimauchi, H.: Population biomass, feeding, respiration and growth rates, and carbon budget of the  
1110 scyphomedusa *Aurelia aurita* in the Inland Sea of Japan, *J. Plankton Res.*, 27(3), 237–248,  
1111 doi:10.1093/plankt/fbh172, 2005a.

1112 Uye, S. and Shimauchi, H.: Population biomass, feeding, respiration and growth rates, and carbon budget of the  
1113 scyphomedusa *Aurelia aurita* in the Inland Sea of Japan, *J. Plankton Res.*, 27(3), 237–248,  
1114 doi:10.1093/plankt/fbh172, 2005b.

1115 Vogt, M., O'Brien, C., Peloquin, J., Schoemann, V., Breton, E., Estrada, M., Gibson, J., Karentz, D., Van  
1116 Leeuwe, M. A., Stefels, J., Widdicombe, C. and Peperzak, L.: Global marine plankton functional type biomass  
1117 distributions: *Phaeocystis* spp., *Earth Syst. Sci. Data*, 4(1), 107–120, doi:10.5194/essd-4-107-2012, 2012.

1118 West, E. J., Pitt, K. A., Welsh, D. T., Koop, K. and Rissik, D.: Top-down and bottom-up influences of jellyfish  
1119 on primary productivity and planktonic assemblages, *Limnol. Oceanogr.*, 54(6), 2058–2071,  
1120 doi:10.4319/lo.2009.54.6.2058, 2009.

1121 Widmer, C. L.: Effects of temperature on growth of north-east Pacific moon jellyfish ephyrae, *Aurelia labiata*  
1122 (Cnidaria: Scyphozoa), *J. Mar. Biol. Assoc. United Kingdom*, 85(3), 569–573,  
1123 doi:10.1017/S0025315405011495, 2005.

1124 Yamamoto, J., Hirose, M., Ohtani, T., Sugimoto, K., Hirase, K., Shimamoto, N., Shimura, T., Honda, N.,  
1125 Fujimori, Y. and Mukai, T.: Transportation of organic matter to the sea floor by carrion falls of the giant  
1126 jellyfish *Nemopilema nomurai* in the Sea of Japan, *Mar. Biol.*, 153(3), 311–317, doi:10.1007/s00227-007-0807-  
1127 9, 2008.

1128